

Volcanic lateral collapse processes in mafic arc edifices

Romero, Jorge E.; Polacci, Margherita; Watt, Sebastian; Kitamura, Shigeru; Tormey, Daniel; Sielfeld, Gerd; Arzilli, Fabio; La Spina, Giuseppe; Franco, Luis; Burton, Mike; Polanco, Edmundo

DOI:

[10.3389/feart.2021.639825](https://doi.org/10.3389/feart.2021.639825)

License:

Creative Commons: Attribution (CC BY)

Document Version

Publisher's PDF, also known as Version of record

Citation for published version (Harvard):

Romero, JE, Polacci, M, Watt, S, Kitamura, S, Tormey, D, Sielfeld, G, Arzilli, F, La Spina, G, Franco, L, Burton, M & Polanco, E 2021, 'Volcanic lateral collapse processes in mafic arc edifices: a review of their driving processes, types and consequences', *Frontiers in Earth Science*, vol. 9, 639825.
<https://doi.org/10.3389/feart.2021.639825>

[Link to publication on Research at Birmingham portal](#)

General rights

Unless a licence is specified above, all rights (including copyright and moral rights) in this document are retained by the authors and/or the copyright holders. The express permission of the copyright holder must be obtained for any use of this material other than for purposes permitted by law.

- Users may freely distribute the URL that is used to identify this publication.
- Users may download and/or print one copy of the publication from the University of Birmingham research portal for the purpose of private study or non-commercial research.
- User may use extracts from the document in line with the concept of 'fair dealing' under the Copyright, Designs and Patents Act 1988 (?)
- Users may not further distribute the material nor use it for the purposes of commercial gain.

Where a licence is displayed above, please note the terms and conditions of the licence govern your use of this document.

When citing, please reference the published version.

Take down policy

While the University of Birmingham exercises care and attention in making items available there are rare occasions when an item has been uploaded in error or has been deemed to be commercially or otherwise sensitive.

If you believe that this is the case for this document, please contact UBIRA@lists.bham.ac.uk providing details and we will remove access to the work immediately and investigate.



Volcanic Lateral Collapse Processes in Mafic Arc Edifices: A Review of Their Driving Processes, Types and Consequences

Jorge E. Romero^{1*}, Margherita Polacci¹, Sebastian Watt², Shigeru Kitamura³, Daniel Tormey⁴, Gerd Sielfeld⁵, Fabio Arzilli¹, Giuseppe La Spina¹, Luis Franco⁶, Mike Burton¹ and Edmundo Polanco⁷

¹ Department of Earth and Environmental Sciences, The University of Manchester, Manchester, United Kingdom, ² School of Geography, Earth and Environmental Sciences, University of Birmingham, Birmingham, United Kingdom, ³ Faculty of Education, Niigata University, Niigata, Japan, ⁴ Catalyst Environmental Solutions, Santa Monica, CA, United States, ⁵ Geociencias, Escuela de Ingeniería, Pontificia Universidad Católica de Chile, Santiago, Chile, ⁶ Observatorio Volcanológico de los Andes del Sur, Servicio Nacional de Geología y Minería, Temuco, Chile, ⁷ Servicio Nacional de Geología y Minería, Santiago, Chile

OPEN ACCESS

Edited by:

Chiara Maria Petrone,
Natural History Museum,
United Kingdom

Reviewed by:

Matteo Roverato,
Université de Genève, Switzerland
Raffaello Cioni,
University of Florence, Italy

*Correspondence:

Jorge E. Romero
jorge_eduardom@hotmail.com

Specialty section:

This article was submitted to
Volcanology,
a section of the journal
Frontiers in Earth Science

Received: 09 December 2020

Accepted: 15 April 2021

Published: 12 May 2021

Citation:

Romero JE, Polacci M, Watt S, Kitamura S, Tormey D, Sielfeld G, Arzilli F, La Spina G, Franco L, Burton M and Polanco E (2021) Volcanic Lateral Collapse Processes in Mafic Arc Edifices: A Review of Their Driving Processes, Types and Consequences. *Front. Earth Sci.* 9:639825. doi: 10.3389/feart.2021.639825

Volcanic cones are frequently near their gravitational stability limit, which can lead to lateral collapse of the edifice, causing extensive environmental impact, property damage, and loss of life. Here, we examine lateral collapses in mafic arc volcanoes, which are relatively structurally simple edifices dominated by a narrow compositional range from basalts to basaltic andesites. This still encompasses a broad range of volcano dimensions, but the magma types erupted in these systems represent the most abundant type of volcanism on Earth and rocky planets. Their often high magma output rates can result in rapid construction of gravitationally unstable edifices susceptible both to small landslides but also to much larger-scale catastrophic lateral collapses. Although recent studies of basaltic shield volcanoes provide insights on the largest subaerial lateral collapses on Earth, the occurrence of lateral collapses in mafic arc volcanoes lacks a systematic description, and the features that make such structures susceptible to failure has not been treated in depth. In this review, we address whether distinct characteristics lead to the failure of mafic arc volcanoes, or whether their propensity to collapse is no different to failures in volcanoes dominated by intermediate (i.e., andesitic-dacitic) or silicic (i.e., rhyolitic) compositions? We provide a general overview on the stability of mafic arc edifices, their potential for lateral collapse, and the overall impact of large-scale sector collapse processes on the development of mafic magmatic systems, eruptive style and the surrounding landscape. Both historical accounts and geological evidence provide convincing proofs of recurrent (and even repetitive) large-scale (>0.5 km³) lateral failure of mafic arc volcanoes. The main factors contributing to edifice instability in these volcanoes are: (1) frequent sheet-like intrusions accompanied by intense deformation and seismicity; (2) shallow hydrothermal systems weakening basaltic rocks and reducing their overall strength; (3) large edifices with slopes near the

critical angle; (4) distribution along fault systems, especially in transtensional settings, and; (5) susceptibility to other external forces such as climate change. These factors are not exclusive of mafic volcanoes, but probably enhanced by the rapid building of such edifices.

Keywords: edifice instability, landslide, unloading, decompression, volcanic geomorphology, debris avalanche, lateral collapse, basaltic volcanism

INTRODUCTION

Lateral collapses (also called “sector” or “flank” collapses) involve gravity-driven, deep-seated destructive removal of volcanic materials (i.e., hundreds of m in depth) from a volcanic edifice, with or without association to an eruption, showing a wide variety of volumes and mobility. These processes share similar attributes (e.g., deposits with similar morphology and texture) to other terrestrial landslides of non-volcanic origin (Siebert, 2002). However, their initiation is often related to seismic processes or magmatic eruptions, and involve long-term (at kyr timescales) modifications of the volcanic system and its immediate environment. Collapses can occur in any type of volcano, but by far the largest number of lateral collapses have been identified at arc stratovolcanoes and large intraplate volcanic islands (Siebert, 2002; Blahút et al., 2019; Watt, 2019). Lateral collapses produce characteristic scars with a wide opening angle and often non-parallel sidewalls (thus affecting a sector of the cone), and often encompass the volcano summit. Their deposits, often forming blocky and heterogeneous debris avalanche deposits (VDAD) can mobilize several cubic kilometers of rock (Bernard et al., 2021), with the largest volumes identified offshore volcanic islands (McGuire, 1996; Oehler et al., 2005; Blahút et al., 2019). Both lateral collapses and their deposits have killed ~3,500 people since 1600 AD, in at least nine catastrophic events, and their direct impacts have been documented between 1 and 20 km from the volcanic source (Auken et al., 2013; Brown et al., 2017; Siebert and Roverato, 2021). During just the twentieth century, it is estimated that 741 people were killed and 267 injured directly by collapse processes, while 4,600 became homeless and about 29,000 were evacuated (Witham, 2005) as a consequence of this phenomenon. Moreover, tsunamis directly generated by lateral collapses have killed many thousands more people (Day et al., 2015): some prominent examples include the 1741 collapse of Oshima-Oshima volcanic island (Japan; volume of 2.5 km³ and ~1,500 fatalities; Satake, 2007); the 1792 collapse of Unzen-Mayuyama (Japan; volume of 0.3 km³ and 15,135 deaths; Sassa et al., 2016); and the 1888 tsunami caused by the collapse of Ritter Island (Papua New Guinea, with a volume from 2.4 to 4.2 km³ and likely causing several thousand deaths on the coastlines of surrounding islands; Watt et al., 2019). More recently, on 22 December 2018, the SW flank of the Anak Krakatau volcano (Indonesia) dramatically collapsed into the sea generating tsunami waves up to 13 m-high along the coast of Sumatra and Java, killing 437 people (Grilli et al., 2019) and triggering a series of violent phreatomagmatic eruptions observed on 23 December 2018 (Walter et al., 2019; Williams

et al., 2019). All of these historical examples occurred on arc volcanoes of relatively small to moderate dimensions, in a global context, and yet their consequences were devastating. Moreover, many of these examples occurred in young (e.g., Anak Krakatau), morphologically simple (e.g., conical forms, such as Ritter) volcanoes, characterized by a limited, mafic compositional range, and with eruptive styles dominated by effusive and minor-explosive activity, rather than large explosive eruptions of viscous, evolved magma. Given that structural failure is commonly linked to hydrothermal alteration, loading and gravitational spreading (van Wyk de Vries and Francis, 1997; Zimbelman et al., 2005; Karstens et al., 2019), and other factors promoting structural weakness (such as intrusion of highly viscous magma; Reid et al., 2010), it may be expected that both age and overall dimensions are significant indicators of susceptibility to failure. However, the above examples illustrate that relatively young, structurally simpler mafic edifices may be just as prone to lateral collapse. The rationale of this review is thus to examine failures in this broad category of “mafic” arc volcanoes, to elucidate the processes driving failure, and to examine if there are specific factors that may drive collapse in these volcanoes, or collapse is simply associated with the same range of processes leading to collapse across other volcanic landforms.

Mafic volcanism, and specifically eruption of basaltic magma, is a widespread volcanic manifestation in our Solar System, extending through different scales and geological times in the evolution of the rocky planets and their natural satellites (Carr, 1973; Strom et al., 1975; Head and McCord, 1978; Walker et al., 1979; Greeley and Spudis, 1981; Campbell et al., 1984; Crisp, 1984; Head et al., 1992, 2008, 2011; Wilson, 2007; Braden et al., 2014). More than a half of the Earth's volcanoes are fed completely or largely by basaltic magmas, and they are found in every type of tectonic environment (Walker and Sigurdsson, 2000). In this sense, at least 42% of the total number of arc stratovolcanoes have either basaltic, basaltic andesite or trachybasalt-trachyandesite dominant compositions; the population living within 30 km from these volcanoes is 44 million, while 388 million live within 100 km (Figure 1; Global Volcanism Program, 2013). Eruption rates tend to be higher in mafic volcanoes than at intermediate to silica-rich volcanic systems (White et al., 2006), which favors relatively rapid edifice construction, and this potentially leads to gravitationally unstable conditions (Baloga et al., 1995; Siebert, 2002; Barrett et al., 2020; Zernack and Procter, 2021) and even to repetitive failure. Volcano instability is also enhanced by a variety of internal (i.e., magmatic intrusions, hydrothermal processes and gravitational load) and external conditions (e.g., climate, erosion and substratum weakness) (McGuire, 1996; Roverato et al., 2021). Lateral collapse in gently sloping basaltic edifices (such as large

shield-like volcanoes at hot-spot settings) has been documented in detail within the last decades and has provided evidence about the largest collapse deposits on the Earth ($\sim 10^3 \text{ km}^3$; McGuire, 1996; Oehler et al., 2005; Blahut et al., 2019). However, understanding how the factors controlling edifice stability and failure processes relate to the dominant magma compositions characterizing a particular volcano, and how this varies across tectonic settings or is influenced by eruption styles, internal structures and the magmatic plumbing system, is still a topic of debate and significant investigation.

This review is intended to establish a connection between the nature of mafic arc volcanism (Figure 1) and volcanic instability, and, using a variety of case studies, to provide a comprehensive typology of the occurrence, impact (on both magmatic systems and volcano surroundings) and post-collapse reactivation of volcanic activity related to large-scale lateral collapses on these volcanoes. This review is not intended to cover sector collapses in volcanic islands of hot spot settings, which have been treated in detail in recent publications (McGuire, 1996; Oehler et al., 2005, 2008; McGuire, 2006; Boulesteix et al., 2012, 2013; Blahut et al., 2019; Di Muro et al., 2021a,b), and are out of the focus of this review on mafic arc volcanoes. Also, we provide just a brief description of other types of landslides affecting mafic volcanoes (smaller, i.e., $<0.1 \text{ km}^3$), originated by surface sliding of slope materials rather than deep-seated flank failures (i.e., sector collapses).

THE CONSTRUCTION AND INTRINSIC INSTABILITIES OF MAFIC EDIFICES IN ARC SETTINGS

Mafic volcanic landforms include both monogenetic and polygenetic volcanoes, which may be all observed in arc settings. Monogenetic volcanoes (formed by single continuous or polycyclic eruptions) are the simplest structures, while polygenetic mafic volcanoes (i.e., erupting more than once during their lifetime) represent centralized venting of magma over time scales of 10^3 – 10^7 years, and can develop complex feeding pathways to the surface from significant depths in the crust (Figures 2A,B; Jerram and Bryan, 2015). Many of these volcanoes are basaltic, in a strict sense, being volumetrically dominated by the eruption of basaltic magmas. However, other volcanoes, including both monogenetic and polygenetic types, may involve similar eruption styles (effusive eruption of relatively low-viscosity lavas; accompanied by minor to moderate explosive eruption styles dominated by Hawaiian to violent-Strombolian activity), but involving magmas that are slightly more silica- or alkali-rich. We thus group such volcanoes under a broader term of mafic volcanoes. We also note that, in long-lived arc volcanoes, the boundary between a mafic and an intermediate volcano can only be loosely defined, and we simply use the term mafic volcano here to denote a volcano that, based on current exposures, is dominated volumetrically by basaltic/basaltic-andesite compositions. A summary of the characteristics of mafic volcanoes is provided in the detailed works of Walker and Sigurdsson (2000);

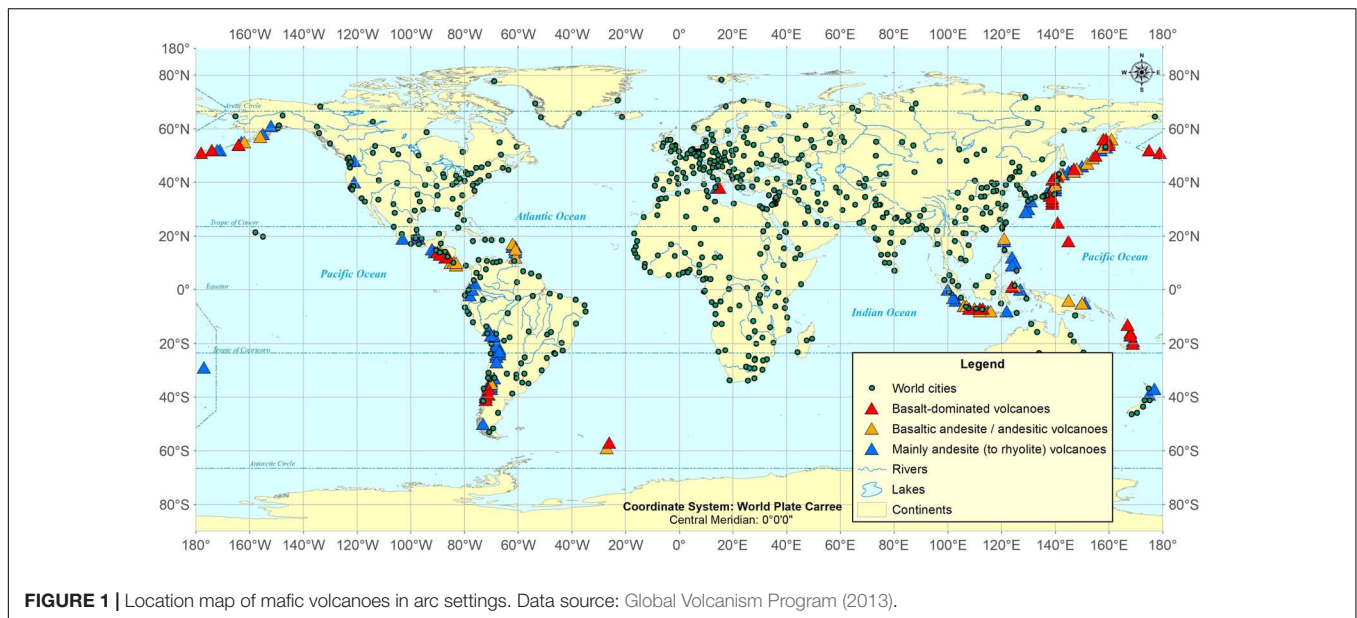
Valentine and Gregg (2008), Valentine and Connor (2015), and Kereszturi and Németh (2012), the latter two focused on monogenetic basaltic volcanoes specifically.

Small-Volume ($<1 \text{ km}^3$) Monogenetic Edifices

Monogenetic mafic volcanoes are represented by purely magmatic edifices such as spatter cones (Figure 3A), cinder cones (Figure 3B), and fissures (Figure 3C), but also by hydrovolcanic structures (maars, tuff rings, and tuff cones; Figure 3D). These volcanoes have volumes normally $<0.1 \text{ km}^3$, rarely up to 1 km^3 , and their maximum slope angles are $\sim 30^\circ$ for cinder cones and $>30^\circ$ for spatter cones (Vespermann and Schmincke, 2000; Németh and Kereszturi, 2015). The largest monogenetic edifices are represented by pyroclastic (cinder) cones, which reach about 300 m height and 900 m in basal diameter (Németh and Kereszturi, 2015). Due to the rapid accumulation of pyroclastic materials, spatter cones may suffer small landslides as seen during the recent (2021) Geldingadalur eruption (Figure 3E; Reykjanes Peninsula, Iceland). Cinder cones may also develop a horseshoe shape, related to lavas flowing away from one region of the cone, resulting in the continuous drafting of pyroclastic material away from the growing cone (Figure 3F; Valentine and Gregg, 2008; Németh et al., 2011). The rafts are made of bedded fragments from the intact cone, partially disintegrated agglutinate deposits or loose pyroclastic debris blanketed by scoria fallout (Valentine et al., 2006) as clearly seen in Marcath volcano (Figure 3F; Valentine et al., 2017). If sudden, a small scale flank failure of the cone portion may cause the unloading of the shallow plumbing system, producing a change in the eruption style (e.g., enhancing explosivity), as seen in Los Morados scoria cone (Figure 3G; Argentina, Németh et al., 2011) or the Timanfaya eruption (1730–1736) at Mazo volcano (Canary Islands) which triggered a small directed blast as well as forming a debris avalanche deposit covering $1,218 \text{ km}^2$ and extending 1.6 km from the vent (Romero et al., 2020a).

Large Volume Polygenetic Volcanoes ($>1 \text{ km}^3$)

Polygenetic mafic volcanoes may correspond to shield volcanoes (Figure 4A), stratovolcanoes (Figure 4B), or even clusters of volcanic landforms such as basaltic volcanic fields and flood basalts. Basaltic volcanic fields are more frequent in back arc basins (Gribble et al., 1996) and flood basalts almost exclusively occur in hot-spot settings intrinsically related to lithospheric architecture (Sheth, 1999). Polygenetic volcanoes of homogenous mafic composition may have a short-lasting evolution, from a few centuries to several 1,000 years, which is comparable in duration of activity to small shield volcanoes in arc settings, but much shorter-lived than typical andesite-dacite stratocones (10^4 – 10^6 years; Hildreth et al., 1998). In quasi-closed systems, even a protracted storage prior to eruption (~ 25 – $6,000$ years) may not significantly alter the primitive bulk composition of magmas before reaching the surface (Winslow et al., 2020). Mafic volcanoes may also represent an early stage in the development of a longer-lived stratovolcano and its underlying feeder system,



which on longer timescales may become dominated by a broader range of more evolved magmatic compositions. This is the case of young stratovolcanoes like Izalco in El Salvador (began in 1770), Pacaya in Guatemala or Cerro Negro in Nicaragua, all of them with basaltic composition contrasting with other more “mature stratovolcanoes” which are often andesitic or dacitic and show evolution trends that have more silicic eruptions with time (Rose et al., 2010). An arguably similar case is the young basaltic-andesite cone of Anak Krakatau, which has developed since the 1883 eruption and destruction of the rhyo-dacitic Krakatau edifice, elevated eruption rates, driven by a high magmatic flux to the surface and the occurrence of frequent, repeated eruptions (with repose intervals of months to decades) appears to be an important factor driving the rapid construction and consequent flank instability of mafic stratovolcanoes.

In contrast to other hotspot or rift-related basaltic volcanoes, which produce large volumes of lava flows, mafic volcanoes in arc settings are fed by volatile-rich magmas (see Xu et al., 2020 for a detailed description of basaltic magma generation in arc settings): typical volatile contents include H_2O from 2 to 6 wt%, significant CO_2 (as high as 2,500 ppm), S (900–2,500 ppm), and Cl (250–2,500 ppm) (Wallace et al., 2015). This promotes the occurrence of explosive eruptions (Houghton and Gonnermann, 2008) and the deposition of tephra fall and pyroclastic density current (PDC) deposits interbedded with lavas (Figure 4C). Mafic polygenetic arc edifices are usually cone-shaped, many hundreds to thousands of meters above their base, and their flanks steepen upward until approximating the repose angle of clastic deposits (about 33–36°; Figure 4D) (Walker, 1993). In addition, when their altitude favors snow accumulation, ice-clad volcanoes generate abundant volcanoclastic deposits of variable origin that include hydrovolcanic interaction, such as tuff breccias, hyaloclastites, lahar sequences and heterogeneous debris avalanche deposits (VDADs) (Skjelkvåle et al., 1989; Sheth et al., 2009), which are intercalated with moraines to

create complex internal structures. Such features also characterize volcanoes with intermediate compositions, but a significant difference, linked to dominant eruptive styles and the dispersal and accumulation patterns of pyroclastic material, distinguishes mafic polygenetic volcanoes.

Predominantly mafic edifices experience a relatively higher frequency of Hawaiian, Strombolian or lava fountain eruptions (Stern et al., 2007; Houghton and Gonnermann, 2008) thus giving high potential of rapid accumulation of unstable, locally dispersed deposits lying at critical angles in the upper part of the edifice (i.e., spatter agglutinates, thick scoria fall deposits or a’a lavas) with variable mechanical properties and frequent unit boundaries or structural discontinuities. These deposits tend to be gravitationally unstable, and are capable of producing small landslides in the summit area of the active volcano, generating valleys clogged by volcanic and volcanoclastic deposits (Figure 5A). Some historical examples of this process include the 12 January 2013 Stromboli (Italy) landslide ($0.1 \times 10^6 m^3$) which was triggered by high magmatic pressure within the conduit and the weakening of the cone by magma fingering (Calvari et al., 2016), or the crater wall collapse of the young Soputan volcano (Indonesia) on 25–26 October 2007, producing a $0.85 \times 10^6 m^3$ debris avalanche during a VEI 3 eruption (Figure 5B) (Kushendratno et al., 2012). On 27 May 2010, Pacaya (Guatemala) experienced the collapse of materials deposited in a ravine (Figure 5C) after a flank eruption (300 m below the summit), causing both a directed blast and debris avalanche, which were then followed by enhanced explosive activity (the most intense eruption since 1964; Wardman et al., 2012; Bollasina, 2014). More recently, a similar valley-infill collapse at Fuego (Guatemala) on 3 June 2018, affected Barranca Las Lajas (Figure 5D; $15 \times 10^6 m^3$), and the hot avalanche mixed with PDCs traveled about 12 km to San Miguel de los Lotes, killing hundreds of people (Albino et al., 2020). Collapse scars from small-scale landslides of this type have distinctive parallel

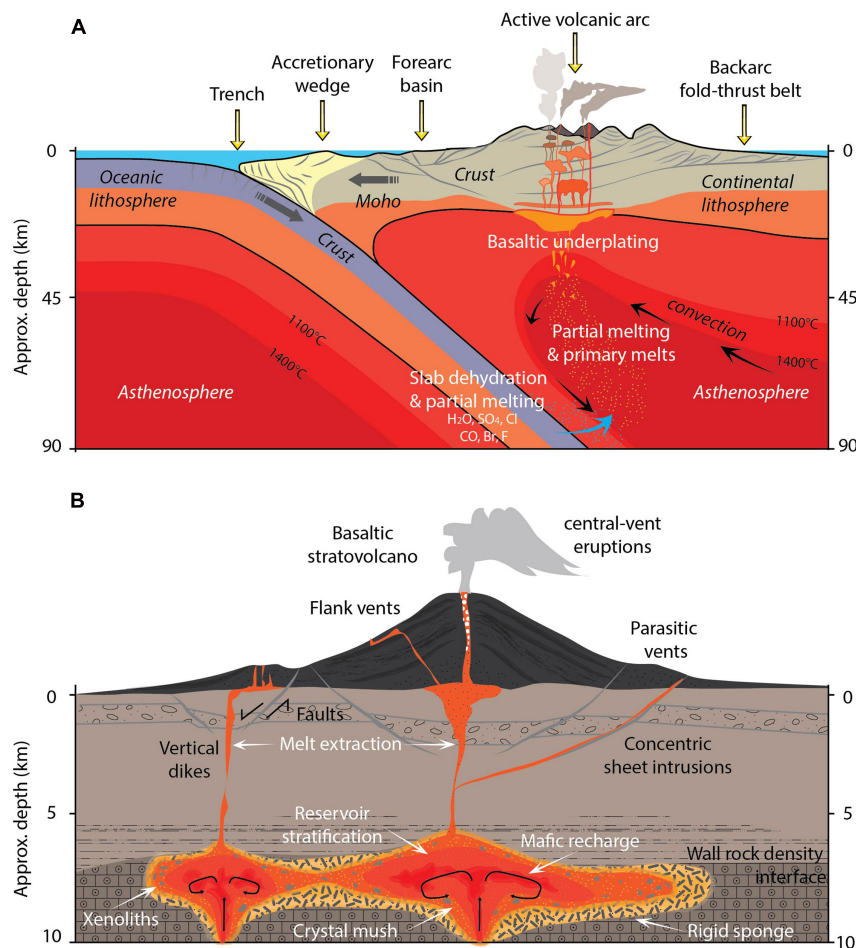


FIGURE 2 | Basaltic volcanism in arc settings. **(A)** Cartoon (not to scale) of the oceanic-continental lithosphere subduction showing the main processes of slab dehydration and generation of partial melts which accumulate below the crust (underplating), then feeding the active volcanism of the overlying arc. Illustration based in Schmidt and Poli (1998). **(B)** Cartoon (not to scale) of the shallow storage and plumbing system of a basaltic volcano.

sidewalls and generally occupy just a small surface in the flanks of the volcano. Other small-scale landslides can be formed by the removal of shallow layers of unstable material producing a flat sliding surface with parallel sidewalls, such as those observed on 30 December 2002 in Stromboli as consequence of a fissure eruption (Figure 5E; $33.5 \times 10^6 \text{ m}^3$; Tinti et al., 2005; Landi et al., 2006; Miraglia, 2006) or by 17 January 2008 in Llaima by spatter collapse (Figure 5F; Romero et al., 2013; Franco et al., 2019). All these different styles of landsliding correspond to shallow-seated landslides, thus encompassing only surficial processes that do not involve a long-term modification of both the internal and external volcanic apparatus, as in the case of lateral collapses.

LATERAL COLLAPSES IN MAFIC ARC VOLCANOES

Sector collapses result from the cumulative effects of different sources of volcanic instability, which increase susceptibility to

failure, potentially in addition to a final triggering event that materializes the failure. Instability factors may be classified in two groups: internal and external. Internal factors include magmatic intrusions, hydrothermal alteration and gravitational deformation (Figure 6A), while external factors are related to the behavior and structural features of the basement (Figure 6B), as well as seismic activity and exogenous processes such as sea-level change and glacial erosion or debuttressing (Figure 6A) (Roverato et al., 2021 and references therein). These factors are not distinct to mafic edifices, but potentially act in all constructional volcanic landforms. Nevertheless, we consider below whether the rapid construction rate and eruption styles typical of mafic volcanoes enhance any of these factors.

Instability Factors

Stratovolcanoes function as high-toughness composite structures made of layers of widely different elastic properties, encouraging fracture deflection and arrest (Gudmundsson, 2012). Therefore, fracture propagation may require less energy in shield-like



FIGURE 3 | Mafic monogenetic volcanoes. **(A)** Spatter Cone (Osorno volcano, Chile); **(B)** Scoria Cone (Villarrica, Chile); **(C)** volcanic fissure (Antuco, Chile); **(D)** Maar (Overo volcano, Chile); **(E)** Sequence of landslide at a spatter cone during the Geldingadalur eruption (Reykjanes Peninsula, Iceland, 2021); **(F)** Marcath volcano (United States) and tephra rafts. **(G)** Los Morados cone (Argentina) and tephra rafts. Photos **(A–C)** by Jorge Romero. Photos **(D–G)** by Gabriel Ureta, Bini Smári, G.A. Vallentine.

volcanoes than in stratovolcanoes, due to their homogeneous internal structure, dominated by lava flows. Despite this, mafic arc stratovolcanoes are expected to be more or less homogeneous in comparison to volcanoes with a wider compositional range and different types of volcanic deposits/products (domes,

coulees, block, and ash flows, etc.) as consequence of similar erupted products along their lifetime and construction. The application of regional or local stress fields in rocks may produce deformation, failure or changes in the physical properties of such rocks (**Supplementary Table 1**; Schön, 2015).

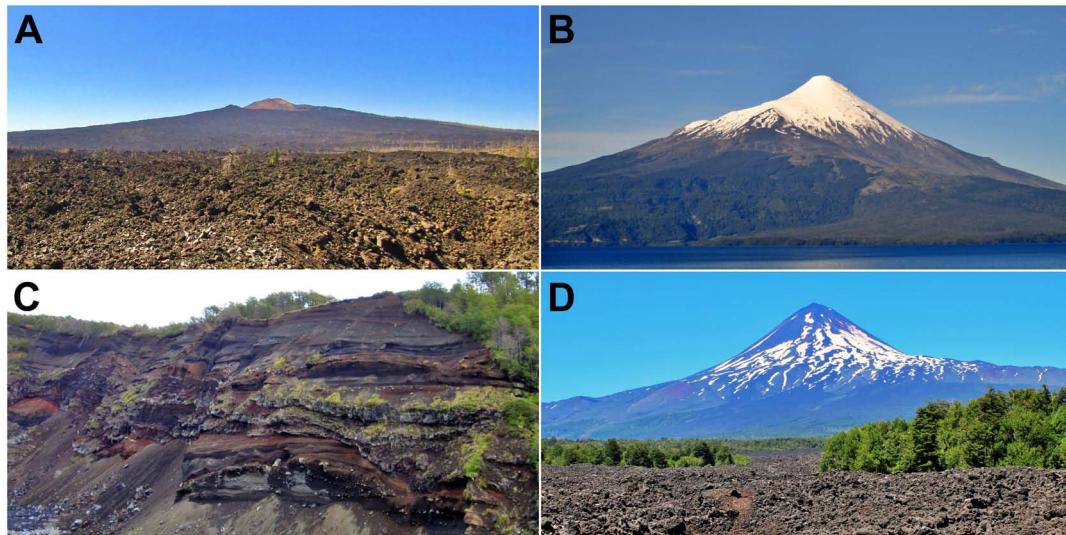


FIGURE 4 | Geomorphology of basaltic polygenetic volcanoes. **(A)** Belknap crater, a shield volcano (OR, United States). **(B)** Osorno stratovolcano (Chile). **(C)** Interbedded pyroclastic deposits and lava flows at Villarrica volcano (Chile). **(D)** Steep slopes of Laima compound volcano (Chile). Photos by Jorge Romero.

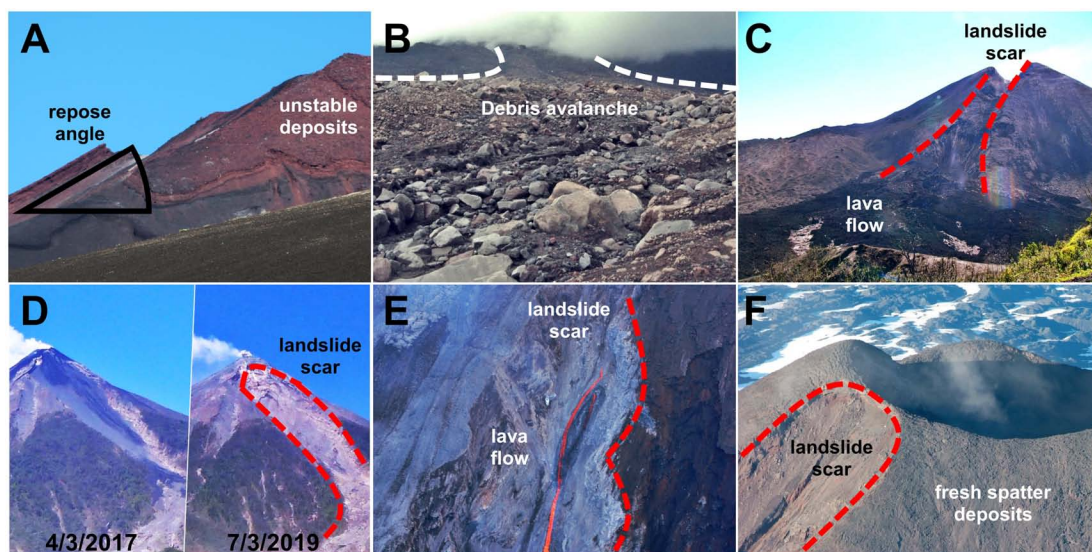


FIGURE 5 | Small landslides in mafic volcanoes. **(A)** Instable spatter and tephra fall deposits in the upper part of Lonquimay volcano, Chile; **(B)** Debris avalanche deposit produced by a landslide in Soputan volcano (October 2007), Indonesia; **(C)** Partial summit and gully collapse at Mackenney cone (Pacaya 2010, Guatemala) and at **(D)** Fuego volcano (2019; Guatemala); **(E)** Scar produced by the Sciara del Fuoco 2002 landslide in Stromboli (Italy); **(F)** Summit landslide of a spatter deposit in Laima volcano (2008; Chile). Photo **(A)** by Jorge Romero, **(B)** by John Pallister, **(C)** by Gustavo Chigna, **(D)** by Alisa Naismith **(E)** by Mauro Coltelli and **(F)** by Daniel Basualto.

Schaefer et al. (2015) show how the strength of basaltic rocks in stratovolcanoes may be modified: it decreases with porosity, increases with strain rate, increases with ambient temperature, and is unsystematically varied by thermal stressing, and due to prolonged loading/unloading (i.e., repeated dike intrusion or inflation/deflation cycles) suggesting these rocks may not behave entirely elastically and accumulate damage, inducing mechanical hysteresis (change in mechanical response as consequence of previous maximum loading). This behavior is not different to that

observed in other intermediate silica rocks (e.g., dacites at Mt. Saint Helens; Kendrick et al., 2013). In terms of their geological strength index (Marinos and Hoek, 2000), basalts from Pacaya may vary between very good (mainly unweathered fresh lavas) to very poor, such as pyroclasts (Schaefer et al., 2013).

Internal Factors

Although dikes are found of all magma compositions, by far the most common and volumetrically significant dikes are basaltic in

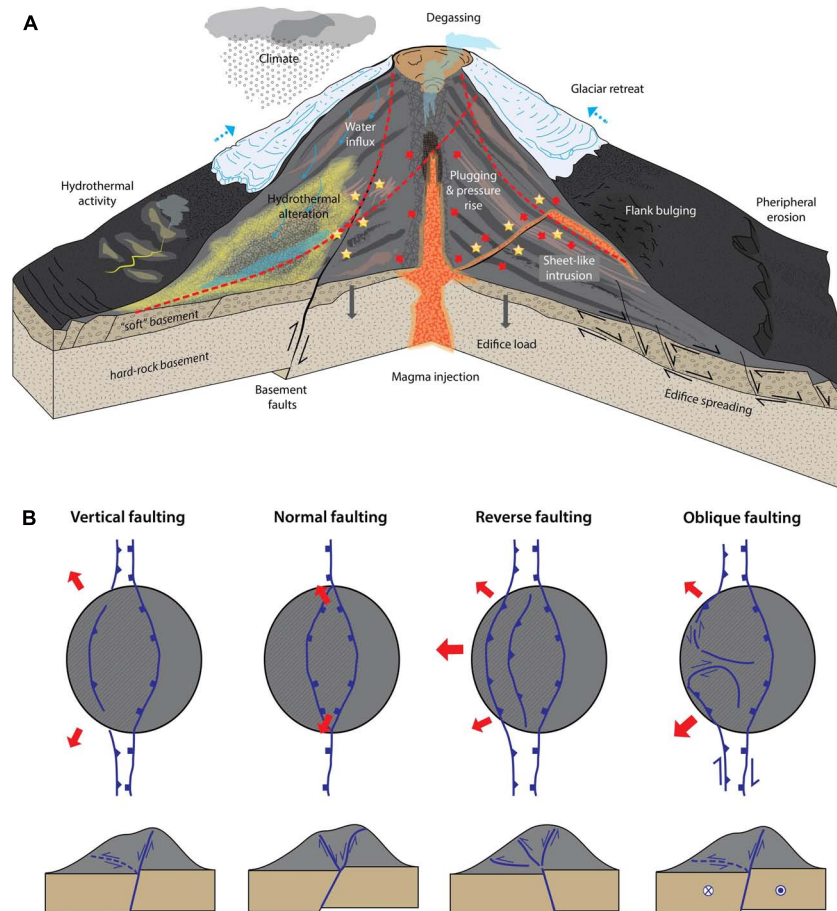


FIGURE 6 | Instability of mafic polygenetic volcanoes. **(A)** Cartoon (not to scale) illustrating the different internal and external sources of instability. Potential slide planes are red dashed lines, while seismicity and deformation are indicated by yellow stars and red arrows, respectively; **(B)** Styles of basement faulting and corresponding styles of collapse at volcano edifices (modified from Mathieu et al., 2011).

composition (Jerram and Bryan, 2015). Polygenetic mafic systems are commonly fed by arrangements of radial or sub-parallel mafic dikes (**Figures 7A,B**), frequently sourcing monogenetic flank eruptions or fissure events, but also central-vent eruptions (**Figure 2C**; Hildreth et al., 1998; Keating et al., 2008; Rose et al., 2010; Gudmundsson, 2012; Gudmundsson et al., 2014; Harp and Valentine, 2018). Magmatic intrusions, especially dikes, are an important source of instability, since they produce deformation, seismicity and release of mechanical (i.e., expansive) and thermal (i.e., heating) energy. This can increase pore fluid pressures, acting on potential basal failure planes and decreasing strength (**Figure 6A**; Elsworth and Voight, 1996; Norini and Acocella, 2011; Hacker et al., 2017). Despite thermal pore fluid pressure changes acting faster than their mechanical counterparts, the latter have a more significant impact on the strength drop (Elsworth and Voight, 1996). Earthquakes may be induced by pore fluid pressure variations caused by dike intrusions (Elsworth and Voight, 1995). In this sense, dike intrusion during modern eruptions of basaltic volcanoes has led to moderate magnitude (M_w 4–6) seismicity (Liu et al., 2018; Williams et al., 2019; Ágústssdóttir et al., 2019), but occasionally these earthquakes may

reach $M_w > 7$ (Chen et al., 2019). During the December 2018 eruption of Etna, a dike intruding in the eastern flank caused spreading (see section “External factors” for spreading; Bonforte et al., 2019). Magma intruded within the sedimentary cover on top of the broad intrusive mesh, generating a transient velocity increase consistent with stress propagation on the unstable flank, and culminating, a few days later, with a magnitude $M_w = 4.9$ earthquake on the Fiandaca–Pennisi Fault (10 km SE from the eruption fissure; Giampiccolo et al., 2020). Thus, increased magma supply rate, preferential intrusion orientation parallel to the maximum regional stress or even intrusion through pre-existing fault planes may promote flank failure (Siebert, 1984; Tibaldi, 2004; Famin and Michon, 2010; Giampiccolo et al., 2020; Hickey et al., 2020). In Cumbre Vieja volcano (Canary islands), dikes of a meter in thickness, but with significant length (> 1 km) may cause flank destabilization (Elsworth and Day, 1999).

The temporary development of shallow intrusions (such as shallow sheet-like intrusions within a few hundreds of meters in depth, **Figure 7C**) is also able to produce flank deformation and collapse (Tormey et al., 1995; Solaro et al., 2010). Deep magma intrusions may also produce edifice deformation and

enhanced sliding, as observed during eruptive cycles in Etna, Stromboli (both in Italy), and Cumbre Vieja (Canary Islands; Walter et al., 2005; Bonaccorso et al., 2011; Alparone et al., 2013; Nolesini et al., 2013; González and Palano, 2014). Events of cryptodome formation, such as that observed during the 1980 Mt. Saint Helens collapse (Reid et al., 2010) are uncommon in mafic volcanoes given the comparatively lower viscosity of basaltic or basaltic andesite magmas [see Leshner and Spera (2015) for additional physical and physico-chemical properties of basaltic magmas], but cannot be discarded as in some volcanoes highly crystalline basalts are found (Kushendratno et al., 2012; Fox, 2019). The exact same factors related to deep magma intrusion and edifice deformation may act at mafic volcanoes in the same way as in volcanoes with wider compositional range.

Hydrothermal alteration is widely known as an instability factor for the lateral collapse of volcanoes (Delmelle et al., 2015). Studies carried out in andesitic arc stratovolcanoes point to acid-sulfate alteration (i.e., smectite, alunite, kaolinite \pm pyrite, and gypsum) as a main indicator of structural weakening (Zimbelman et al., 2005 and references therein). Similar processes are likely to occur in mafic volcanic edifices (Navarre-Sitchler et al., 2009). According to Moon and Jayawardane (2004), the early stages of basalt weathering (fresh to slightly weathered) consist of a rapid reduction in both CaO and MgO concentrations without major mineralogical change, but with a dramatic loss of strength (~43% of bearing capacity). Weathering also involves loss of cations and disruption of mineral lattice structures, and with more extensive weathering, secondary clay minerals form. The loss of shear strength will be a function of the type of alteration (related to T and pH) rather than the amount or degree of alteration (del Potro and Hürlimann, 2009), and in basaltic lava and pyroclasts it may vary between -45 and -85% (Pola et al., 2014). Low-T hydrothermal alteration products of basalts (i.e., <300°C) include smectites, zeolites, calcium silicates, calcite, pyrite, and quartz (Kristmannsdóttir, 1979): mineral assemblages that would result in structural weakening of the affected rocks. Geophysical surveys have imaged hydrothermal systems at large mafic arc stratovolcanoes such as Fuji (Japan), Llaima or Osorno (Chile) at shallow levels (~1 km), with kilometric extension inside or below the edifice (Aizawa et al., 2005; Franco et al., 2019; Díaz et al., 2020), indicating the possible presence of hydrothermally altered cores inside these edifices. These cores may deform under gravitational deformation producing a series of surface landslides before, during and after the main flank failure event (Cecchi et al., 2004). Thus, there is good evidence that a very similar range of hydrothermal alteration and weakening processes can apply in mafic edifices, in the same way that occurs in edifices dominated by other compositions. Indeed, the rates of such weathering may commonly be high in mafic edifices, particularly those characterized by a vigorous hydrothermal system.

Volcanoes that are particularly unstable are those with weak zones represented by intense silica-clay alteration, active acid lakes and/or solfataras fields (Figure 7D; van Wyk de Vries et al., 2000; Cecchi et al., 2004; Delmelle et al., 2015) commonly related to hydrovolcanic and glaciovolcanic interactions. Mafic ice-capped or tropical volcanoes, such as Copahue, Planchón (Both in Chile-Argentina) or Poás (Costa

Rica) can develop persistent intracrater acid and clay alteration (Rodríguez and van Bergen, 2017; Báez et al., 2020; Romero et al., 2020b) in this way. However, other mafic volcanoes with persistent magmatic influx such as Villarrica (Chile), Etna or Stromboli (Italy) have only developed a weak or peripheral hydrothermal system, which respond to magmatic intrusions and seasonal meteoric waters (Finizola et al., 2003; Ortiz et al., 2003; Liotta et al., 2010). Such systems are less prone to being extensively affected by hydrothermal alterations, and it is not therefore simply the case that a high magmatic flux and elevated thermal gradient within an edifice is associated with more active or more extensive hydrothermal alteration.

Rapid edifice building, typical of mafic stratovolcanoes in arc settings, normally means the generation of significant height differences above the surroundings (2–4 km), constructional processes that outpace erosion, and the development of typically steep slopes (30–40° for stratovolcanoes and cinder cones). These volcanoes may be active during hundreds of years (e.g., Sangay erupting since at least 1628 AD or Villarrica since ~1400 AD; Monzier et al., 1999; van Daele et al., 2014). As consequence of persistent eruptions at mafic, they constitute many of the largest continental volcanic edifices (e.g., Semeru and Slamet, Indonesia; Fuji, Japan; Etna, Italy; Arenal, Costa Rica; and Llaima and Villarrica in Chile, etc.). These all act to increase flank instability (Ponomareva et al., 2006), and are factors promoted by the elevated magmatic flux and frequent eruptions that characterize many mafic arc systems.

Under gravitational load, volcanoes may also develop “spreading” or outward edifice displacement, and “sagging”, which implies inward displacement (Borgia, 1994; Merle and Borgia, 1996). Spreading promotes summit extension and basal constriction (Figure 6A), potentially forming incipient flank instabilities (Karstens et al., 2019), while sagging will produce inner thrusting, constricts the upper edifice and thus impedes magma rise. Within their “lifetime”, some volcanoes may experience a full cycle of deformation processes (Borgia, 1994) which may overlap, repeat, or be omitted: building, sagging, intruding (magmas trapped in the base of the edifice) and spreading. Such factors may be important in volcanoes of all types and compositions, but again the rapid construction characteristic of many mafic systems potentially exacerbates the influence of spreading and loading effects. Spreading is also promoted by external factors, such as a weak basement (substratum), and will be detailed in the next section.

External Factors

External factors may not be expected to differ substantially between mafic edifices and those of other compositions, unless the factors are promoted in specific volcano-tectonic settings that are also characterized by mafic volcanism. The geometry and type of substratum controls basal edifice spreading in continental environments, and spreading is possible if (1) there is a weak layer in the substratum (Figure 6A; evaporates, marls, clays, hydrothermally altered rocks or shales, or poorly consolidated marine sediments), (2) the thickness of the brittle layer above the weak layer is relatively thin, and (3) the volcano is not buttressed on all sides (Merle and Borgia, 1996). Excellent

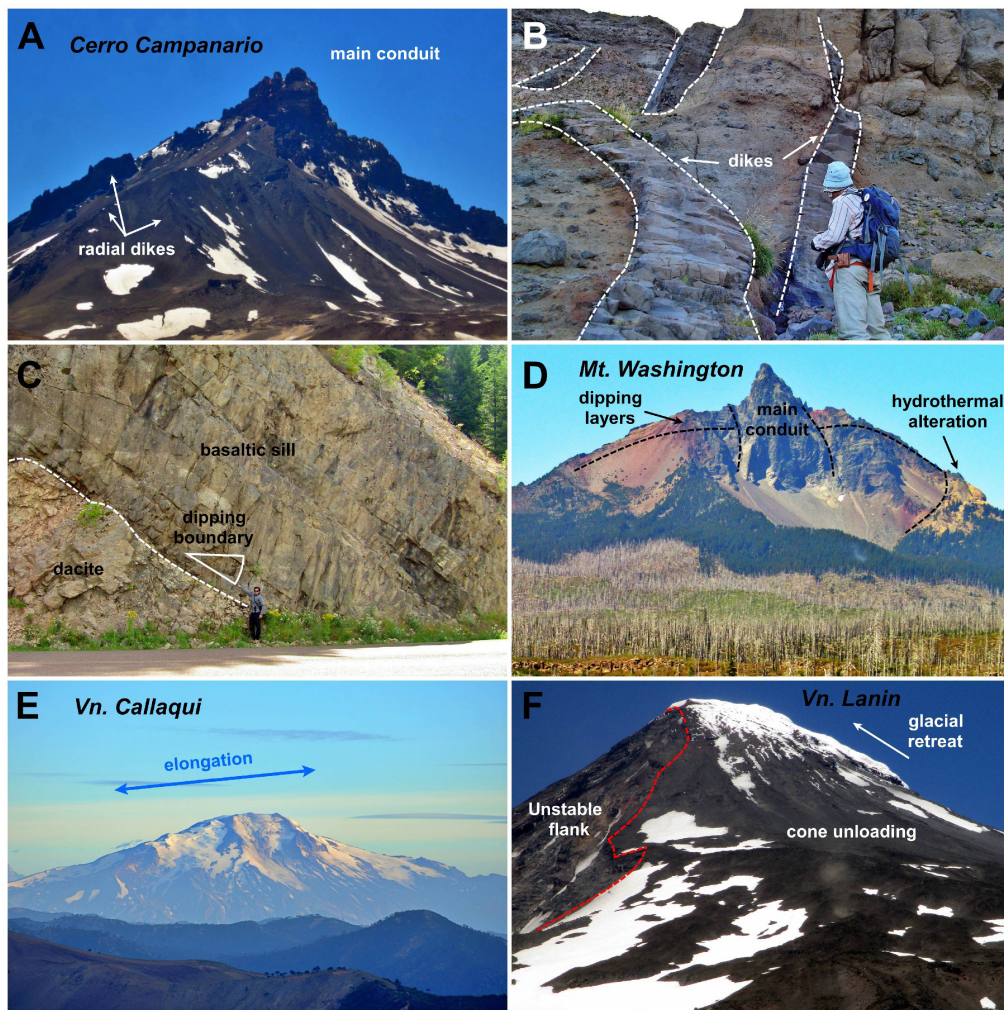


FIGURE 7 | Internal architecture of basaltic edifices. **(A)** Cerro Campanario and its radial dikes Chile; **(B)** Basaltic dikes intruding volcaniclastic sequences in the flanks of Callaqui volcano, Chile; **(C)** Basaltic sill intruding Cenozoic dacitic units at Clearwater Overlook, Washington (United States); **(D)** Internal structure and peripheral hydrothermal alteration at Mt. Washington (Cascades of Oregon, United States), a basaltic shield edifice; **(E)** Elongation of Callaqui volcano (Chile), lying over a transtensional fault system; **(F)** Glacial retreat at Lanin volcano (Chile), exposing the volcano structure (causing unloading) and increasing flank instability. Photos **(B)** by Gerd Siefeld and the rest by Jorge Romero.

examples of spreading are found in Mombacho (Nicaragua; van Wyk de Vries and Francis, 1997), Mt. Iriga (Philippines; Paguican et al., 2012), Mt. Usu (Japan, Goto and Tomiya, 2019), and probably the volumetrically largest in Socompa (Chile, van Wyk de Vries et al., 2001) with 35 km³ of VDAD. There is limited evidence supporting spreading at mafic arc edifices, however, this process has been described in Ritter Island (Papua New Guinea; Karstens et al., 2019), and the lower slopes of Mt. Etna (Acocella et al., 2003; Lundgren et al., 2004; Solaro et al., 2010; Bonforte et al., 2011), as indicated by the growth of anticline structures, while the spreading is probably driven by deeper magma injection. In contrast, spreading has been widely reported in large-sized volcanic islands, where the underlying sediments form a low-viscosity decollement which results in the formation of rift zones, generally triangular, producing flanks prone to sliding (Walter and Troll, 2003; Münn et al., 2006).

Possible explanations for the lack of documented spreading at mafic arc edifices are that (1) a weak substratum is not especially common in arc settings and (2) mafic arc volcanoes have comparatively smaller volumes than larger edifices with a broader compositional range (and smaller than intraplate volcanic islands), and as such, spreading is a less significant factor in many mafic settings.

Arc volcanism is associated with extensional, compressional, strike-slip or oblique motions; the structure of the arc does control the volcanic output through different processes, even though extension (also in strike-slip and compressional arcs) is directly related to output rate (Acocella and Funicello, 2010). A review of volcanism in compressional settings (Tibaldi et al., 2009) demonstrates that active intra-arc fault systems commonly control the position of volcanic centers and contribute to a causal relationship between magmatism and thermal weakening

of the upper crust (de Saint Blanquat et al., 1998). For instance, within arc fault systems, strike-slip domains favor the production of less hydrous magmas, limit crustal assimilation and shorten residence times, hence producing more mafic volcanism than occurs in contractional/transpressional settings, as can be found along the Southern Andean volcanic zone (SAVZ) or Eastern Anatolia (Tibaldi et al., 2009). The transtensional Liquiñe-Ofqui Fault System in the SAVZ hosts numerous stratovolcanoes dominated by basaltic and basaltic andesitic products (e.g., Planchón, Callaqui, Llaima, Antillanca, Osorno, Hornopirén, and Apagado volcanoes). Here, Andean transverse faults play a role in the distribution of basaltic lavas: Most late Pleistocene and Holocene volcanic centers defining NE-trending alignments, including both composite stratovolcanoes and minor eruptive centers, contain mainly basaltic to basaltic andesite lithologies (e.g., Osorno–Puntiagudo–Cordón Cenizos volcanic chain in the Southern Andes), while NW-trending fractures and faults have more evolved compositions, including rhyolites (Stern et al., 2007; Cembrano and Lara, 2009; Bucchi et al., 2015; Pérez-Flores et al., 2016; Sielfeld et al., 2019). This is in contrast to the Indonesian volcanic arc, where the Sumatra Fault has limited control on volcanic processes, distribution and size (Acocella et al., 2018). These crustal fault intersections represent highly permeable zones for fluid circulation and magmatic intrusion (Piquer et al., 2019; Norini et al., 2020; Pearce et al., 2020), but also transfer structural instabilities to the overlying edifice. The role of the regional tectonic regime and the collapse of stratovolcanoes has been studied for decades (Moriya, 1980; Francis and Wells, 1988; Tibaldi, 1995; Lagmay et al., 2000; Wooller et al., 2009; Mathieu et al., 2011; Paguican et al., 2012), and as is illustrated by the examples above, is a potentially significant control on both the construction and failure of mafic edifices, just as in edifices dominated by broader or more evolved compositional ranges.

Particular collapse directions might be influenced by basement fault interactions, such as fault intersections and complex fault damage zone architectures. In general, for volcanoes lying over normal faults, the fault will propagate through the edifice and produce a shallow graben, which will constrain instability to be nearly parallel, not perpendicular to the fault strike (**Figure 6B**; Wooller et al., 2009) and the collapse is in favor of the downthrown block (**Figure 6B**; Vidal and Merle, 2000). Vertical and thrust faulting favors landslides normal to the fault strike (**Figure 6B**; van Wyk de Vries and Davies, 2015). Significant instability directed normal to thrust fault strike is most likely to develop when a fault is sited beneath a peripheral flank, where it is able to destabilize a large portion of the edifice (Wooller et al., 2009; Paguican et al., 2012). Volcanic edifices lying over strike-slip fault systems usually generate a pair of sigmoidal faults (one reverse and another normal; **Figure 6B**) with a “flower-like” structure (folded structures associated with strike-slip faults) inside the edifice which allows magma intrusion and promotes instability (Lagmay et al., 2000). Collapse areas are normal to the strike of the dike injections and affect the cone flanks subject to extension (Mathieu et al., 2011). In summary, the role of basement faults seems to be the same for volcanoes of different compositions, with the exception that some transtensional tectonic settings favor the occurrence of mafic

volcanoes, as aforementioned. In transtensional tectonic regimes such as these typically controlling mafic volcanism in the SAVZ or Indonesia, volcanic edifices are prone to growth following elongated architectures (as result of the overall feeder dikes geometry), but these elongated edifices may increasingly lead to normal-to-the-volcano-elongation steeper flanks, triggering avalanches and flank erosion (e.g., Callaqui volcano in Chile, **Figure 7E**; Polanco and Naranjo, 2008; Sielfeld et al., 2017).

Climate and the related erosive forces may also play a role in volcanic instability (**Figure 7F**; Roberti et al., 2021), at both long and immediate time-scales. However, this is a field in progress and subject to active discussion, and it is not clear whether there are particular factors that would make these processes more or less significant in mafic versus other settings, except for the fact that the often relatively smaller dimensions and younger age of mafic edifices may reduce the overall importance of edifice erosion in influencing lateral collapse. Several works (Keating and McGuire, 2004; Capra, 2006; Quidelleur et al., 2008; Roverato et al., 2011, 2015; Tost and Cronin, 2016) suggest that major inter-eruptive lateral collapses were absent during glacial climax, but started immediately during glacial retreat and sea level rise. Some of this evidence (Capra, 2006) is subject to the new geochronologic constrains and the finding of other different triggering mechanisms at these case studies (van Wyk de Vries et al., 2001; Clavero et al., 2008; Clavero and Godoy, 2010; Jicha et al., 2015).

Triggering Mechanisms

Earthquakes frequently trigger landslides on the Earth (Keefer, 2002), however, volcanic seismicity is generally characterized by lower-magnitude events (M 2–3) than tectonic seismicity, and moderate-to-large volcanic earthquakes ($M \geq 4.5$) are relatively scarce (Zobin, 2001). In volcanoes lying above seismically active tectonic faults, those faults can produce earthquakes as large as Mw 6.0 or 7.0 and can trigger near-field landslides, i.e., ~10 km radius from the epicenter (Sepúlveda et al., 2010; Lastras et al., 2013; Piquer et al., 2019) or even the flank failure of the edifice. Despite this, the 1980 collapse of Mt. Saint Helens was initiated by an M 5 earthquake (Malone et al., 1981).

Intense meteorological events or important variations in the climate do trigger lateral collapses (Crandell, 1989; Scott et al., 1995, 2005; Vallance and Scott, 1997; Capra, 2006; Roverato et al., 2011; Capra et al., 2013; Farquharson and Amelung, 2020), such as during the 1998 Casita alkali-basalt volcano landslide (Nicaragua), which was initiated by hurricane Mitch precipitations and killed 2,513 people (Scott et al., 2005), but the intense weathering played a key conditioning role in the volcano instability (Kerle et al., 2003).

Collapse Dimensions and Geometry

Small-scale lateral collapses ($0.2\text{--}1.0\text{ km}^3$) are frequent in mafic arc stratovolcanoes, and they involve a narrow sector of the volcano or a part of one flank producing characteristic U or V-shaped scars in plan view. This is the case of the lateral collapses in Callaqui (Chile) and Pacaya 1 ka BP (Guatemala). For Callaqui, its $>320 \pm 70\text{ BP}$ collapse (0.69 km^3) only affected a portion

of the NW flank, and was probably triggered by a structurally-controlled magmatic intrusion as indicated by dikes parallel to the collapse scar (Sielfeld et al., 2017), which may have suddenly depressurized producing a thin PDC deposit directly overlying the avalanche (Polanco and Naranjo, 2008). On Pacaya, the lateral collapse (0.65 km^3) occurred during an ongoing eruption and affected mostly the SW flank and the top of the edifice (**Figure 8A**), producing then a full sequence of directed blasts and scoria fallout (Kitamura and Matías, 1995; Vallance et al., 1995). More recently, Anak Krakatau collapsed on 22 December 2018 removing c. 50% of the subaerial extent of the island (**Figure 8B**), estimated at $0.22\text{--}0.3 \text{ km}^3$ (Walter et al., 2019). Despite the relatively small volume of these avalanches, they have traveled tens of kilometers from their source, and their occurrence is relatively common at small volume mafic volcanoes.

Large sector collapses ($>1.0 \text{ km}^3$) are events that destroy a great extent of the edifice including its summit and part of the basement underlying the cone. Sector collapses cut deeply enough into the edifice to involve multiple rock units, and the resulting collapse scar is generally horseshoe-shaped in plan view with diameters of a few kilometers. Historical collapses of basaltic to basaltic andesitic arc stratovolcanoes include the 1741 Oshima-Oshima Island (**Figure 8C**; Japan) and the 1888 Ritter Island failures (Papua New Guinea). Satake and Kato (2001) calculated the total volume of Oshima-Oshima VDAD as 2.5 km^3 , with a total run out of 16 km from the island, producing a deadly tsunami with about 2,000 fatalities (Satake, 2007). 147 years later, Ritter Island produced the largest historically recorded lateral collapse and removed $2\text{--}4 \text{ km}^3$ of the cone but mobilized up to 13 km^3 of material by eroded and deformed seafloor plus distal turbidites (Day et al., 2015; Karstens et al., 2019). A similar scale (c. 2.9 km^3) sector collapse affected Sajaka I edifice (**Figure 8D**; Aleutians) $<5 \text{ ky BP}$ destroying nearly a half of the edifice and producing a collapse scar of 1.5-km-diameter (Coombs et al., 2007). Geologic records provide abundant evidence on several sector collapses of other mafic volcanoes during the Holocene. For instance, Antuco volcano (Chile), produced a 5 km^3 VDAD between 6 and 4 ky BP involving the loss of c. 1 km of height of the cone, leaving a remarkable 4-km-diameter scar (**Figure 8E**; Moreno et al., 2000; Clavero and Godoy, 2010; Martínez et al., 2018; Romero et al., 2021). During the Pleistocene, mafic edifices of Mt. Kanaton and Adagdak island (Aleutians) collapsed, the first forming a 5-km-diameter horseshoe caldera where N. Kanaga volcano has reconstructed inside; VDAD extends 30 km N, with volume $\sim 25 \text{ km}^3$ (Waythomas et al., 2003; Coombs et al., 2007; Montanaro et al., 2011). The VDAD of basaltic Adagdak volcano (**Figure 8F**) is poorly constrained and reaches 33 km of run-out and 12.5 km wide, with c. 35-m-thickness (Montanaro et al., 2011). Repetitive sector collapses are also frequent at some basaltic volcanoes, such as Gareloi (Aleutians), which shows three large submarine VDADs to the N, NW, and E, from which one of them (NW; Unknown age) is 8.3 km^3 and is sourced from a 6.5 km wide submarine scar (Montanaro et al., 2011). This situation has been also reported in subaerial volcanoes of Kamtchatka: Kambalani has collapsed at least three times between 6.3 and 6.0 ky BP producing VDADs totaling $5\text{--}10 \text{ km}^3$, while Late Pleistocene Zarechny volcano experienced at least two

major collapses to southeast involving 6–8 and $0.5\text{--}0.7 \text{ km}^3$ of the edifice, respectively (Ponomareva et al., 2006). This evidence is diagnostic of a relevant susceptibility of such mafic volcanic edifices to collapse, even several times during their evolution, mainly as consequence of rapid growth. However, mafic edifices do span the same volume and mobility fields than volcanoes with other compositions as seen in **Figure 9**.

Characteristics of Debris Avalanche Deposits

Irrespective of the composition of the collapsed volcano, VDADs are composed of detritic volcanic material, i.e., coherent, consolidated or poorly consolidated fragments of the volcanic edifice (Glicken, 1991). They correspond to chaotic breccias, with extremely variable grain size (size from a few micrometers to blocks $>10 \text{ m}$), and a main sandy grain size, without internal structures (**Figure 6A**; Leyrit, 2000). Blocks (blocks are $1\text{--}100 \text{ m}$ size; megablocks are $>100 \text{ m}$ size; **Figure 10A**) and clasts (clasts are $2 \text{ mm}\text{--}1 \text{ m}$ size; megaclasts are $>1 \text{ m}$) use to show jigsaw cracks (**Figure 10B**) and the matrix ($1 \mu\text{m}\text{--}2 \text{ mm}$ size) forms mixed facies when combined with clasts (**Figure 10C**), or matrix facies if it represents the dominant fraction in the deposit (Dufresne et al., 2021). The surface of the deposit is usually hummocky (**Figure 10D**; Ui, 1983; Bernard et al., 2021; Dufresne et al., 2021). VDADs are described in terms of their characteristic facies (Ui, 1983; Glicken, 1991, 1996; Palmer et al., 1991; Capra et al., 2002; Scott et al., 2001; Roverato et al., 2011; van Wyk de Vries and Davies, 2015; Dufresne et al., 2021). The mobility of VDADs can be expressed as H/L ratio (height loss v/s run out distance, i.e., coefficient of friction).

In Guatemala, La Democracia (Late Pleistocene) and Late Holocene Pacaya VDADs are characterized by hummocky surface, and volumes of 2.4 and 0.65 km^3 , respectively. La Democracia contains exclusively mafic clasts (basalts and basaltic andesites), and hummocks are up to 40 m high, mainly distributed in the margins of the deposit (Vallance et al., 1995). The Pacaya VDAD (**Figure 10A**) is also characterized by mixed facies containing homogeneous basaltic jigsaw-fit blocks, disturbed pyroclastic sequences and pumices incorporated by the ingestion of pre-collapse ignimbrites in a sandy-grain size matrix and hummocks with heights between 5 and 15 m (Kitamura and Matías, 1995; Vallance et al., 1995). Another two massive basaltic-andesite VDADs are recognized at Sangay volcano; older-S1, $250\text{--}100 \text{ ka}$, and younger-S2, about 30 ka, and they involve 29 and 32.5 km^3 of material, from which S2 is among the most significant volcanic avalanches in the world associated with continental arc volcanoes (Valverde et al., 2021). In S2 at least 541 hummocks have been identified and they have heights of $2\text{--}40 \text{ m}$, with largest sizes observed at $40\text{--}50 \text{ km}$ from the vent (*ibid*). The presence of hummocks, block facies and metric jigsaw-fit clasts is also characteristic at the small volume (0.69 km^3) $320 \pm 70 \text{ BP}$ VDAD of Callaqui (Polanco and Naranjo, 2008). Another remarkable example corresponds to the mafic VDADs of Kambalani volcano (Kamtchatka; 6.3 and 6.0 ky BP) which contain containing mafic lava blocks and splintered scoria, which are supported in a minor amount of matrix, facies with dominant clay-sized material and a

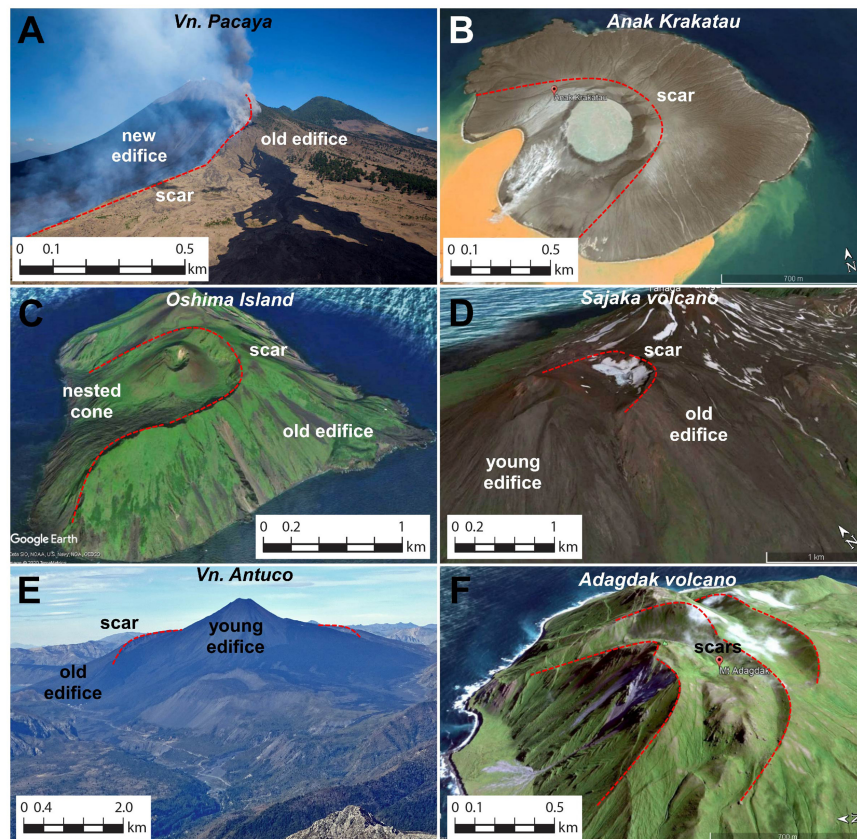


FIGURE 8 | Morphological features related to sector collapses in basaltic volcanoes **(A)** Pacaya volcano (Guatemala); **(B)** Anak Krakatau (Indonesia); **(C)** Oshima-Oshima volcano (Japan); **(D)** Sakaja volcano (Aleutians); **(E)** Antuco volcano (Chile), and **(F)** Adagdak volcano (Aleutians) with multiple collapse scars. Individual authors of selected field photos are indicated in the figure. Red dashed lines show the scar of these collapses. Photo **(A)** by CONRED, and **(E)** by Constanza Jorquera. **(B–D,F)** image source is Google Earth.

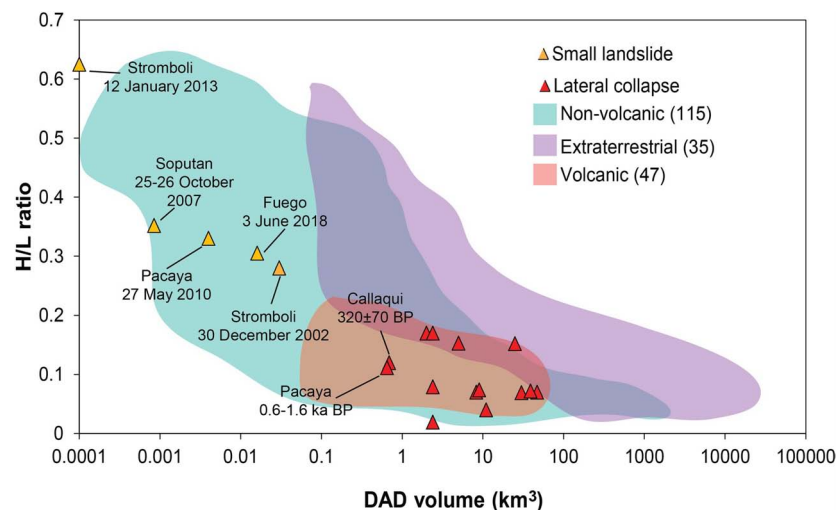


FIGURE 9 | Plot of the H/L ratio v/s volume for VDAD deposit sourced from basaltic volcanoes. The field for non-volcanic and planetary landslides is indicated. The plot and fields are modified from van Wyk de Vries and Davies (2015). Original data is found in **Supplementary Table 2**. All small landslides in mafic volcanoes fall in the field of non-volcanic landslides, while all sector collapses are in the same field than any other sector collapse irrespectively of the composition of the failed volcanic edifice.

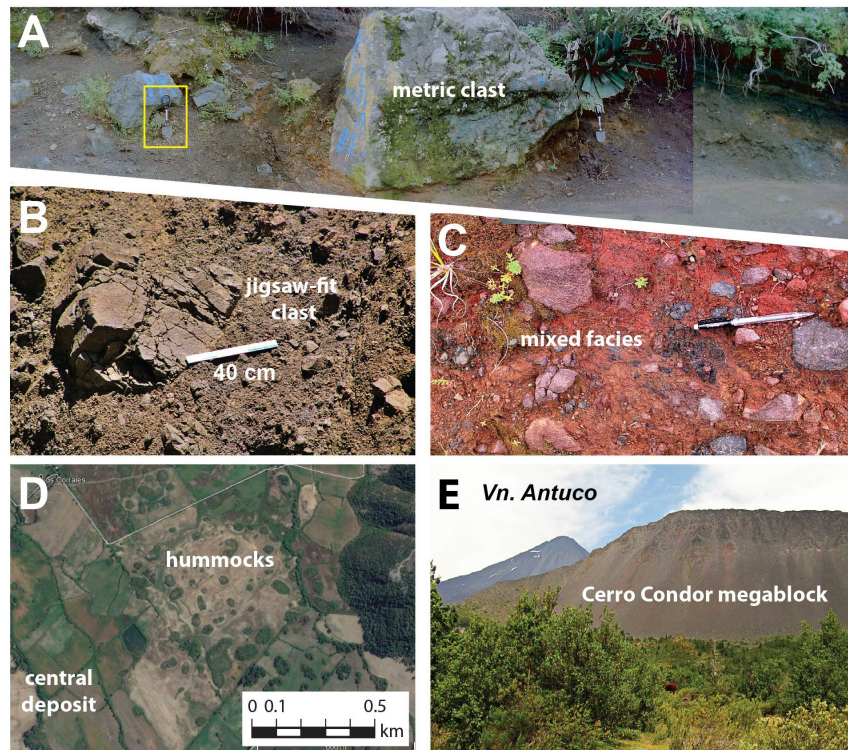


FIGURE 10 | Debris avalanche deposits (DADs). **(A)** VDAD from Pacaya (Guatemala) 1 kyr BP sector collapse, with the presence of metric clasts. Scale shovel indicated by the yellow square. **(B)** Jigsaw-fit clast and **(C)** matrix facies of the Antuco (Chile) VDAD. Hummocky surface left by the 90–20 kyr BP sector collapse of Planchón volcano (Chile). **(E)** Kilometric megablock (toreva) of the Antuco volcano sector collapse (Chile). Photo **(A)** was provided by Shigeru Kitamura and photos **(B–E)** by Jorge Romero.

zone enriched in pumice clasts picked up from older ignimbrites (Ponomareva et al., 2006). The youngest of these deposits is directly overlaid by a mafic PDC deposits. In Japan, two well-studied VDADs sourced from dominantly mafic volcanoes provide good constraints on their overall characteristics: The c.16 ka Zenkoji deposit from Usu volcano (0.3 km^3 ; Goto and Tomiya, 2019) and the 2.9 ky BP Gotemba debris avalanche deposit (Goda; 1.76 km^3) from Mt. Fuji (Miyaji et al., 2004). Zenkoji VDAD has hummocky surface and reaches 6.5 km of subaerial run out, entering the sea; block facies dominate, and jigsaw-fit blocks correspond to pre-collapse basaltic andesite from Usu, ignimbrite and fluvial fragments ingested from the soft basement (Goto and Tomiya, 2019). Gotemba VDAD resulted from the collapse of Ko-Fuji (Older Fuji; Japan) and is composed of blocks, showing jigsaw cracks, along with smaller blocks ranging from several tens of centimeters up to 1 m in diameter, with a matrix composed of a mixture of smaller pieces of blocks and ash-sized materials, all of them corresponding to altered gray basaltic lava, weathered tephra including red scoria and white clay (Miyaji et al., 2004). This deposit has also a hummocky surface, reaching 24 km in distance and its H/L is estimated at 0.113 (**Supplementary Table 2**; Yoshida et al., 2012). It seems the presence of megablocks (intact fragments of the collapsed edifice) is not common, however, the VDAD of Antuco volcano (7.0–4.0 cal. ky BP, c. 5 km^3) develops a toreva/block facies in the most proximal

region ($<4 \text{ km}$ distance from the vent; **Figure 10E**), in part represented by a kilometric fragment named “Cerro Condor”, while at larger distances the avalanche develops mixed facies and matrix facies with jigsaw fragments and metric blocks (Lohmar, 2000; Moreno et al., 2000; Clavero and Godoy, 2010; Romero et al., 2021). From the statistical comparison of both Zenkoji and Gotemba deposits with other five andesitic VDADs, by analysis the size distribution of hummocks with distance from the source, the data show little or no difference between them, thus suggesting similar physical characteristics despite compositional variations and size distribution only correlated to the mobility of the avalanche (Yoshida et al., 2012). In this sense, the most important factor in controlling flow mobility is the proportion of fine grained material (Masson et al., 2002) which in turn is related to the nature of the failed volcanic edifice: volcanoes with higher proportions of pyroclastic materials will allow greater run-out distances than those mainly composed of lava. We can assume that mafic volcanoes may have a considerable proportion of tephra in the edifice; however, this condition is also present in many intermediate or acid volcanoes, and does not constitute a significant difference.

Depending on the confinement of the avalanche, the resultant VDAD deposits may distribute their facies in a longitudinal arrangement with a proximal-to-distal textural variation (when confined to valleys), or display a fan-like arrangement of facies

at open areas (see Palmer et al., 1991). With an exceptional high mobility, the Río Teno VDAD (Planchón) is a unique case study as the fall height is estimated at 3,700 m and a run out distance of 95 km, with an H/L of 0.03 (Naranjo et al., 1999; Scott et al., 2001; Tormey, 2010). This deposit is confined to a narrow Andean valley draining to the west, and the majority of hummocks are distributed in the margins of the channelized flow, and at the extensive fan formed at the foothills of the Andes (McPhail, 1973; Naranjo et al., 1999).

Data collected within this work (**Supplementary Table 2; Figure 9**) show both landslides and sector collapses in mafic volcanoes display a reverse correlation between their H/L values and the volume of DADs (10^5 – 10^{10} m³; **Figure 9**); H/L values for small landslides range between 0.3 and 0.6, while typical sector collapses vary from 0.03 to 0.17. This relationship implies a greater mobility of those debris masses with increasing slid volume, and has no significant difference with VDADs from volcanoes with other geochemical compositions rather than mafic ones.

Overall Impacts

Syn- and Post-collapse Eruptive and Magmatic Activity

The pressure drop caused by sector collapses (Manconi et al., 2009) may trigger eruptions by either sudden decompression of the hydrothermal system, shallow magma or by initiation of renewed magma ascent (Watt, 2019), but also to suppress an ongoing eruption (Pinel and Albino, 2013). For instance, “Bandai-type” collapses are entirely non-magmatic in nature, but may be accompanied by phreatic explosions as hydrothermal system is decompressed; non-juvenile tephra fallouts (10^6 – 10^8 m³) are typically emitted, and then the activity can be followed by magmatic or phreatomagmatic eruptions. This may be the case of Antuco, where the VDAD does not contain juvenile material, but diluted PDCs overlie the collapse sequence (Moreno et al., 2000; Romero et al., 2021).

The effect of decompression in hydrous basaltic melts includes volatile (i.e., H₂O and CO₂) oversaturation, degassing, crystallization and cooling (Pichavant et al., 2013; Arzilli et al., 2015, 2019 and references therein). Isothermal (T of 1,025°C) basaltic andesite rapid magma decompression experiments (from 150 MPa to 100, 65, 42, 21, and 10 MPa) of Shea and Hammer (2013) show that the crystallizing textures are comparable to those observed by cooling. Crystallinity may reach ~30% below 40 MPa, with an important effect on magma rheology, thus affecting degassing efficiency, and finally affecting explosivity (Lindoo et al., 2017; Arzilli et al., 2019). Apart from the crystal fraction, bubble nucleation also affects magma rheology (rigid spherical bubbles increase bulk viscosity while deformable bubbles reduce it; Giordano, 2019). One of the most immediate volcanic phenomena related to the rapid decompression of shallow magma during a sector collapse may be a blast (if a collapse occurs during an eruption or when magma is within the shallow conduit), which is caused by the rapid collapse of an inclined explosive column resulting from instantaneous decompression initiated by lateral collapse. Blasts form relatively

dense, density-stratified and grain-size-stratified PDC (Belousov et al., 2007). As blasts require high viscosity magmas to be formed (i.e., andesitic to rhyolitic; Belousov et al., 2020) there are very few examples in mafic systems, and such processes may, in general, be more common in volcanic systems characterized by more evolved magmas. They may, however, occur in basaltic systems erupting high-crystallinity magma (Kitamura and Matías, 1995; Vallance et al., 1995; Natland and Atlas, 2003; Pallister et al., 2012).

Available examples of mafic syn-collapse magmatic eruptions include Secche di Lazzaro phreatomagmatic eruption (Stromboli) and its related PDCs during the Neostromboli sector collapse (6 ky BP) (Bertagnini and Landi, 1996; Giordano et al., 2008; Petrone et al., 2009), the 1888 collapse of Ritter Island followed by a powerful submarine explosive eruption triggered by collapse (Papua New Guinea; Watt et al., 2019), or the 23 December 2018 collapse of Anak Krakatau (Williams et al., 2019), which was immediately followed by intense surtseyan eruptions with an elevated magma flux and gas release relative to typical historical eruptions (Gouhier and Paris, 2019). Additional evidence of syn-collapse explosive activity, constrained by the existence of pyroclastic deposits directly overlying VDADs, is found in Sajaka and Kanaga (Aleutians), Oshima-Oshima island in Japan, Pacaya 1 ka (Guatemala), where an ongoing Strombolian eruption (unit Pc-t5a) became more intense after the lateral collapse (c. 0.6 km³) (Kitamura and Matías, 1995; Vallance et al., 1995; Coombs et al., 2007; Satake, 2007). Another potential case is the 7–4 ka sector collapse of Antuco volcano (Chile; 5 km³) which was apparently followed by a Plinian tephra fallout dispersed eastward, and westward stratigraphy includes massive PDCs and subsequent lava flows (Moreno et al., 2000; Clavero and Godoy, 2010; Romero et al., 2020c). However, classifying these eruptions as “syn-collapse” is a difficult task if the timing of these stratigraphic events is not well constrained.

The extrusion of lava domes or effusive eruptions, soon after a sector collapse without any syn-eruptive activity, are usually called “Unzen-type” or “Mayu-Yama” (Ui, 1989). Again, effusive eruptions of large volume may occur in mafic edifices, in a similar way to those observed in more evolved systems. A good example of this type of collapse may be that of the basaltic Planchón volcano (SAVZ; Chile-Argentina) about 90–20 ky BP, which produced a new volcano (Planchón II) fundamentally formed by basaltic lava flows, some of them up to 19-km-long, right on top the collapsed edifice (Naranjo et al., 1999; Naranjo and Haller, 2002).

Several processes have been recognized as indicators of a response of a magma plumbing system to decompression following lateral collapse (cf. Watt, 2019), including shifts toward more mafic erupted compositions, the eruption of anomalous magma compositions, changes in eruption rates and the migration of vents. Some of these factors may be expected to be less recognizable in mafic systems, given their more restrictive compositional ranges and that they are generally associated with a less well-developed shallow crustal storage and plumbing system (which is the part of a plumbing system likely most strongly influenced by surface loading and unloading associated with edifice growth and destruction; cf. Pinel and Jaupart, 2005;

Pinel and Albino, 2013). Nevertheless, examples such as those at Ritter Island (Watt et al., 2019) and Stromboli (Petrone et al., 2009), cited above, indicate that mafic systems may be just as susceptible as more evolved systems to being modulated by surface loads.

The reorganization of the plumbing system after lateral collapse has been associated with main vent migration and a new arrangement of dikes. Even before collapse, a single outward-creeping flank is sufficient to modify the entire rift architecture of a volcano (Walter and Troll, 2003). In mafic volcanoes, new intrusions will tend to be oriented parallel to the collapse scar following the un-buttressed flank (**Figure 9**; Tibaldi, 2004; Acocella and Tibaldi, 2005); the dikes outside the ridge generally dip outward, while in the collapse scar and along the scar side, there is an important deviation from the ridge trend where dikes are found en échelon and strike oblique to the scar wall (Walter and Troll, 2003; Delcamp et al., 2012, 2018). The location of the main vent usually changes toward the collapse depression (**Figure 9**; Tibaldi et al., 2008; Maccaferri et al., 2017) by deflecting the pathways of magmatic intrusions underneath the volcano, which results in the formation of a new eruptive center within the collapse embayment. Evidence reported from Sajaka, Kanaga, Great Sinkin (all of them in the Aleutians), Planchón (SAVZ), Fuego (Guatemala), and Stromboli (Italy), shows that the shift in the location of the main vent after the sector collapse is commonly in the order of a few hundred meters to a few kilometers (1–3 km) (**Supplementary Table 2**). However, this pattern depends on the local tectonic stress, which may be large enough to mask the unloading effect of the collapse (Maccaferri et al., 2017). Particularly, the Neostromboli cone shows summit, flank and satellite vents and sheet intrusions with different geometry and location through time, reflecting the interplay of regional tectonics, precursory instability processes and volcano load, in addition to petrogenetic changes after its sector collapse (Vezzoli et al., 2014).

In terms of changes to erupted compositions, post-collapse shifts in activity may imply compositional changes driven by magmatic processes related to decompression (**Supplementary table 2**) which result from: (1) renewed replenishment of the reservoir (i.e., its initiation or increase in the supply rate) from a deeper source, or (2) the eruption of denser, and hence primitive, magma which otherwise would have stalled at shallow depth (Pinel and Jaupart, 2005). The effusion of compositionally anomalous lavas (e.g., Ritter Island or Antuco; Watt, 2019; Watt et al., 2019) is explained by mixing between pre-existing melts and renewed mafic inputs. Moreover, a rapid regeneration of the edifice has been reported ($0.6\text{--}10\text{ km}^3/\text{k.y}$) in mafic volcanoes and is accompanied by more mafic products lasting $10^3\text{--}10^4$ years, as in Stromboli, Antuco, Ritter Island, and Oshima-Oshima (Yamamoto, 1988; Tibaldi, 2004; Martínez et al., 2018; Watt, 2019; Watt et al., 2019). Other volcanoes do not show apparent compositional changes, as Planchon II, the products of which are very similar in composition compared to that of Planchón I (pre-collapse). As for other types of edifice, there is not an entirely consistent pattern that has emerged in terms of the magmatic response to collapse in mafic edifices. This response is likely dependent on the spatial organization of the plumbing system

and the status of the system at the time of collapse (e.g., whether shallow, eruptible magma is present), although a similar array of behaviors has been observed across all volcano types.

CONCLUDING REMARKS AND FUTURE RESEARCH

In this review, we have provided evidence on the susceptibility of volcanoes with mafic composition to collapse, with the particular focus on systems dominated by mafic (basaltic and basaltic andesite) products. Small monogenetic volcanoes (i.e., $<1\text{ km}^3$) are unstable due to their rapid building and can produce small landslides affecting their structure, producing characteristic horseshoe-shaped morphologies. In the case of large polygenetic volcanoes ($>1\text{ km}^3$), particularly stratovolcanoes, they experience a comparatively short-lasting evolution ($10^4\text{--}10^6$ years) compared to counterparts of intermediate-to-silicic compositions, and produce both interbedded effusive and explosive deposits with overall homogeneous composition which rapidly accumulate near the vent to produce gravitationally unstable materials. These conditions facilitate the occurrence of small landslides ($<0.1\text{ km}^3$) involving valleys clogged by volcanoclastic materials and unstable carapaces of recently erupted volcanics in the upper part of the cone.

Key characteristics to increase volcanic instability at mafic arc stratovolcanoes are:

- 1 Frequent sheet-like intrusion of magmas in the form of dikes and sills, accompanied by intense deformation and seismicity (up to Mw 7) to increase pore fluid pressure causing strength drop.
- 2 Hydrothermal systems at shallow levels ($\sim 1\text{ km}$) in the edifice, especially at volcanoes with sporadic magma flux and/or geothermal manifestations (e.g., active acid lakes and/or solfataras fields) producing alteration of basaltic rocks with mineral assemblages including smectites, zeolites, calcium silicates, calcite, pyrite, and quartz.
- 3 Large volcanic edifices with slopes near the critical angle ($30\text{--}40^\circ$), built on a weak substratum, with evidence of spreading.
- 4 Volcanoes lying over active tectonic fault systems, especially in transtensional settings, subject to internal extension and magma intrusion through sigmoidal faults, producing unstable flanks normal to the strike of these dikes.
- 5 Volcanic edifices subject to the effects of glacial retreat, tropical storms or intense seismicity.

All of these factors of instability may be also observed in other non-mafic edifices, thus we suggest that these conditions are enhanced by rapid construction in mafic volcanoes, but are not exclusive of mafic volcanoes. In fact, we are not able to say that mafic volcanoes are more prone to collapse than other intermediate or silica rich volcanoes at arc settings, as it will require a detailed research on the relation between sector collapse and the full spectrum of magma compositions.

In this sense, at least a dozen historical cases of sector collapse have been provided for andesite volcanoes by Voight (2000). However, we can conclude that both historical accounts and geological evidence provide convincing proofs of recurrent (and sometimes repetitive) large-scale ($>0.5 \text{ km}^3$) lateral failure of mafic stratovolcanoes, even in short time-scales. Some of these sector collapses involved a volume of tens of km^3 , and produced notable collapse scars of few km wide. The related VDADs are similar in terms of internal architecture, size and mobility to those sourced from intermediate or silicic volcanoes; however, a few continental examples are outstanding in terms of their extension and volume: (1) one of the longest run-outs reported in the literature achieved by the Planchón Teno VDAD (Chile, 95 km; McPhail, 1973; Naranjo et al., 1999) which is an example of a confined debris avalanche (Tost et al., 2015) in Andean Valleys; and (2) two mafic VDADs from Sangay volcano (Ecuador) which are among the most significant in the world, and they reached up to 60 km from the source despite they are unconfined (Valverde et al., 2021). Therefore, it is necessary to assess sector collapse hazard from rapidly growing mafic volcanoes, using field mapping of ancient VDAD deposits, implementing detailed geotechnical evaluations (Voight, 2000; Apuani et al., 2005; del Potro and Hürlimann, 2009; Schaefer et al., 2013, 2015) and carrying out instability monitoring and landslide prediction, as it has been developed for some active mafic volcanoes in the world (Solaro et al., 2010; Intrieri et al., 2013; Nolesini et al., 2013; Poland et al., 2017; Schaefer et al., 2019).

During and after sector collapses, the decompression of volatile-rich basaltic melts may trigger a sequence of paroxysmal explosive eruptions, which may often sample more differentiated products; these deposits have been reported but rarely documented in detail. Comprehensive stratigraphic and geochronologic studies are necessary to better constrain the relationship between these large sector collapses and subsequent explosive eruptions at mafic volcanoes. In addition, coupled petrological observations, numerical and analog models may greatly contribute to assess the decompression effect of basaltic melts under natural conditions modulated by lateral collapses (Di Muro et al., 2021a). Moreover, post-collapse activity is generally related to rapid edifice regeneration by renewed replenishment of the reservoir, accompanied in some cases by changes in the architecture of the plumbing system. Improving the knowledge about these short and long-term reactions of

shallow magmatic systems is fundamental for post-collapse volcano hazard assessment. Comparing these findings with the existing knowledge about sector collapses at oceanic mafic volcanoes may provide a solid framework to understand the logics behind edifice instability, lateral collapse and post-collapse evolution at all mafic volcanoes, with applications even at a planetary scale.

AUTHOR CONTRIBUTIONS

JR conceived the study, compiled, and organized the literature review for this manuscript, and wrote the text. His work was supported and supervised MP, FA, GL, and MB, who also edited the manuscript. SK, SW, DT, EP, GS, and LF provided material for the case studies, and contributed to the manuscript editing. All authors contributed to the article and approved the submitted version.

FUNDING

JR is supported through a Dean's Doctoral Scholar Awards of the University of Manchester and NSFGEO-NERC-funded project DisEqm (NERC Reference: NE/N018575/1) and V-PLUS projects.

ACKNOWLEDGMENTS

The authors are grateful to G. A. Vallentine, G. Chigna, M. Coltelli, D. Basualto, CONRED, C. Jorquera, John Pallisterfor, Alisa Naismith, and Bini Smári supplying some of the photographs contained in the figures. Detailed reviews provided by Matteo Roverato, Raffaello Cioni and the editors Chiara Petrone and Valerio Acocella greatly contributed to improve this manuscript.

SUPPLEMENTARY MATERIAL

The Supplementary Material for this article can be found online at: <https://www.frontiersin.org/articles/10.3389/feart.2021.639825/full#supplementary-material>

REFERENCES

- Acocella, V., and Funicello, F. (2010). Kinematic setting and structural control of arc volcanism. *Earth Planet. Sci. Lett.* 289, 43–53. doi: 10.1016/j.epsl.2009.10.027
- Acocella, V., and Tibaldi, A. (2005). Dike propagation driven by volcano collapse: a general model tested at Stromboli, Italy. *Geophys. Res. Lett.* 32: L08308.
- Acocella, V., Behncke, B., Neri, M., and D'Amico, S. (2003). Link between major flank slip and 2002–2003 eruption at Mt. Etna (Italy). *Geophys. Res. Lett.* 30:2286. doi: 10.1029/2003GL018642
- Acocella, V., Bellier, O., Sandri, L., Sébrier, M., and Pramumijoyo, S. (2018). Weak tectono-magmatic relationships along an obliquely convergent plate boundary: sumatra, Indonesia. *Front. Earth Sci.* 6:3.
- Ágústssdóttir, T., Winder, T., Woods, J., White, R. S., Greenfield, T., and Brandsdóttir, B. (2019). Intense seismicity during the 2014–2015 Bárðarbunga-Holuhraun Rifting event, Iceland, reveals the nature of dike-induced earthquakes and caldera collapse mechanisms. *J. Geophys. Res. Solid Earth* 124, 8331–8357.
- Aizawa, K., Yoshimura, R., Oshiman, N., Yamazaki, K., Uto, T., Ogawa, Y., et al. (2005). Hydrothermal system beneath Mt. Fuji volcano inferred from magnetotellurics and electric self-potential. *Earth Planet. Sci. Lett.* 235, 343–355. doi: 10.1016/j.epsl.2005.03.023
- Albino, F., Biggs, J., Escobar-Wolf, R., Naismith, A., Watson, M., Phillips, J. C., et al. (2020). Using TanDEM-X to measure pyroclastic flow source location, thickness and volume: application to the 3rd June 2018 eruption of Fuego volcano, Guatemala. *J. Volcanol. Geotherm. Res.* 406:107063. doi: 10.1016/j.jvolgeores.2020.107063

- Alparone, S., Bonaccorso, A., Bonforte, A., and Currenti, G. (2013). Long-term stress-strain analysis of volcano flank instability: the eastern sector of Etna from 1980 to 2012. *J. Geophys. Res. Solid Earth* 118, 5098–5108. doi: 10.1002/jgrb.50364
- Apuani, T., Corazzato, C., Cancelli, A., and Tibaldi, A. (2005). Stability of a collapsing volcano (Stromboli, Italy): limit equilibrium analysis and numerical modelling. *J. Volcanol. Geotherm. Res.* 144, 191–210. doi: 10.1016/j.jvolgeores.2004.11.028
- Azzilli, F., Agostini, C., Landi, P., Fortunati, A., Mancini, L., and Carroll, M. R. (2015). Plagioclase nucleation and growth kinetics in a hydrous basaltic melt by decompression experiments. *Contrib. Mineral. Petrol.* 170:55.
- Azzilli, F., La Spina, G., Burton, M. R., Polacci, M., Le Gall, N., Hartley, M. E., et al. (2019). Magma fragmentation in highly explosive basaltic eruptions induced by rapid crystallization. *Nat. Geosci.* 12, 1023–1028. doi: 10.1038/s41561-019-0468-6
- Auker, M. R., Sparks, R. S. J., Siebert, L., Croswell, H. S., and Ewert, J. A. (2013). statistical analysis of the global historical volcanic fatalities record. *J. Appl. Volcanol.* 2, 1–24.
- Báez, A. D., Báez, W., Caselli, A. T., Martini, M. A., and Sommer, C. A. (2020). The glaciovolcanic evolution of the Copahue volcano, Andean Southern Volcanic Zone, Argentina-Chile. *J. Volcanol. Geotherm. Res.* 396:06866.
- Baloga, S., Spudis, P. D., and Guest, J. E. (1995). The dynamics of rapidly emplaced terrestrial lava flows and implications for planetary volcanism. *J. Geophys. Res. Solid Earth* 100, 24509–24519. doi: 10.1029/95jb02844
- Barrett, R., Lebas, E., Ramalho, R., Klauke, I., Kutterolf, S., Klügel, A., et al. (2020). Revisiting the tsunamigenic volcanic flank collapse of Fogo Island in the Cape Verdes, offshore West Africa. *Geol. Soc. Spec. Publ.* 500, 13–26. doi: 10.1144/sp500-2019-187
- Belousov, A., Belousova, M., Hoblitt, R., and Patia, H. (2020). The 1951 eruption of Mount Lamington, Papua New Guinea: devastating directed blast triggered by small-scale edifice failure. *J. Volcanol. Geotherm. Res.* 401:106947. doi: 10.1016/j.jvolgeores.2020.106947
- Belousov, A., Voight, B., and Belousova, M. (2007). Directed blasts and blast-generated pyroclastic density currents: a comparison of the Bezymianny 1956, Mount St Helens 1980, and Soufrière Hills, Montserrat 1997 eruptions and deposits. *Bull. Volcanol.* 69:701. doi: 10.1007/s00445-006-0109-y
- Bernard, B., Takarada, S., Andrade, S. D., and Dufresne, A. (2021). “Terminology and strategy to describe large volcanic landslides and debris avalanches,” in *Volcanic Debris avalanches: from Collapse to Hazard*, eds M. Roverato, A. Dufresne, and J. Procter (Berlin: Springer). doi: 10.1007/s10346-012-0366-0
- Bertagnini, A., and Landi, P. (1996). The Secche di Lazzaro pyroclastics of Stromboli volcano: a phreatomagmatic eruption related to the Sciara del Fuoco sector collapse. *Bull. Volcanol.* 58, 239–245. doi: 10.1007/bf03395970
- Blahút, J., Balek, J., Klimeš, J., Rowberry, M., Kusák, M., and Kalina, J. (2019). A comprehensive global database of giant landslides on volcanic islands. *Landslides* 16, 2045–2052. doi: 10.1007/s10346-019-01275-8
- Bollasina, A. (2014). *The May 2010 Eruption of Pacaya Volcano, Guatemala: an Experimental Study of Subliquidus Magma Rheology*. Columbia: University of Missouri Columbia.
- Bonaccorso, A., Bonforte, A., Currenti, G., Del Negro, C., Di Stefano, A., and Greco, F. (2011). Magma storage, eruptive activity and flank instability: inferences from ground deformation and gravity changes during the 1993–2000 recharging of Mt. Etna volcano. *J. Volcanol. Geotherm. Res.* 200, 245–254. doi: 10.1016/j.jvolgeores.2011.01.001
- Bonforte, A., Guglielmino, F., and Puglisi, G. (2019). Large dyke intrusion and small eruption: the December 24, 2018 Mt. Etna eruption imaged by Sentinel-1 data. *Terra Nova*. 31, 405–412. doi: 10.1111/ter.12403
- Bonforte, A., Guglielmino, F., Coltelli, M., Ferretti, A., and Puglisi, G. (2011). Structural assessment of Mount Etna volcano from permanent scatterers analysis. *Geochem. Geophys. Geosys.* 12:Q2002.
- Borgia, A. (1994). Dynamic basis of volcanic spreading. *J. Geophys. Res. Solid Earth* 99, 17791–17804. doi: 10.1029/94jb00578
- Boulesteix, T., Hildenbrand, A., Gillot, P. Y., and Soler, V. (2012). Eruptive response of oceanic islands to giant landslides: new insights from the geomorphologic evolution of the Teide–Pico Viejo volcanic complex (Tenerife, Canary). *Geomorphology* 138, 61–73. doi: 10.1016/j.geomorph.2011.08.025
- Boulesteix, T., Hildenbrand, A., Soler, V., Quidelleur, X., and Gillot, P. Y. (2013). Coeval giant landslides in the Canary Islands: implications for global, regional and local triggers of giant flank collapses on oceanic volcanoes. *J. Volcanol. Geotherm. Res.* 257, 90–98. doi: 10.1016/j.jvolgeores.2013.03.008
- Braden, S. E., Stopar, J. D., Robinson, M. S., Lawrence, S. J., Van Der Bogert, C. H., and Hiesinger, H. (2014). Evidence for basaltic volcanism on the Moon within the past 100 million years. *Nat. Geosci.* 7, 787–791. doi: 10.1038/ngeo2252
- Brown, S. K., Jenkins, S. F., Sparks, R. S. J., Odbert, H., and Auker, M. R. (2017). Volcanic fatalities database: analysis of volcanic threat with distance and victim classification. *J. Appl. Volcanol.* 6, 1–20. doi: 10.1016/b978-0-12-107180-6.50006-8
- Bucchi, F., Lara, L. E., and Gutiérrez, F. (2015). The Carrán–Los venados volcanic field and its relationship with coeval and nearby polygenetic volcanism in an intra-arc setting. *J. Volcanol. Geotherm. Res.* 308, 70–81. doi: 10.1016/j.jvolgeores.2015.10.013
- Calvari, S., Intrieri, E., Di Traglia, F., Bonaccorso, A., Casagli, N., and Cristaldi, A. (2016). Monitoring crater-wall collapse at active volcanoes: a study of the 12 January 2013 event at Stromboli. *Bull. Volcanol.* 78:39.
- Campbell, D. B., Head, J. W., Harmon, J. K., and Hine, A. A. (1984). Venus: volcanism and rift formation in Beta Regio. *Science* 226, 167–170. doi: 10.1126/science.226.4671.167
- Capra, L. (2006). Abrupt climatic changes as triggering mechanisms of massive volcanic collapses. *J. Volcanol. Geotherm. Res.* 155, 329–333. doi: 10.1016/j.jvolgeores.2006.04.009
- Capra, L., Bernal, J. P., Carrasco-Núñez, G., and Roverato, M. (2013). Climatic fluctuations as a significant contributing factor for volcanic collapses. evidence from Mexico during the Late Pleistocene. *Global Planet. Change* 100, 194–203. doi: 10.1016/j.gloplacha.2012.10.017
- Capra, L., Macias, J. L., Scott, K. M., Abrams, M., and Garduño-Monroy, V. H. (2002). Debris avalanches and debris flows transformed from collapses in the Trans-Mexican volcanic belt, Mexico—behavior, and implications for hazard assessment. *J. Volcanol. Geotherm. Res.* 113, 81–110. doi: 10.1016/s0377-0273(01)00252-9
- Carr, M. H. (1973). Volcanism on mars. *J. Geophys. Res.* 78, 4049–4062.
- Cecchi, E., de Vries, B. V. W., and Lavest, J. M. (2004). Flank spreading and collapse of weak-cored volcanoes. *Bull. Volcanol.* 67, 72–91. doi: 10.1007/s00445-004-0369-3
- Cembrano, J., and Lara, L. (2009). The link between volcanism and tectonics in the southern volcanic zone of the Chilean Andes: a review. *Tectonophysics* 471, 96–113. doi: 10.1016/j.tecto.2009.02.038
- Chen, K., Smith, J. D., Avouac, J. P., Liu, Z., Song, Y. T., and Gualandi, A. (2019). Triggering of the Mw 7.2 Hawaii earthquake of 4 May 2018 by a dike intrusion. *Geophys. Res. Lett.* 46, 2503–2510. doi: 10.1029/2018gl081428
- Clavero, J. E., and Godoy, E. (2010). The late Holocene collapse of Antuco volcano: a valley confined debris avalanche flow, southern Andes, Chile. *Cities Volcanoes Abstracts* 6:42.
- Clavero, J., Godoy, E., Arancibia, G., Rojas, C., and Moreno, H. (2008). *Multiple Holocene Sector Collapses at Calbuco Volcano, Southern Andes*. Abstracts, Poster Session III, IAVCEI General Assembly. Reykjavik, Iceland, 41.
- Coombs, M. L., White, S. M., and Scholl, D. W. (2007). Massive edifice failure at Aleutian arc volcanoes. *Earth Planet. Sci. Lett.* 256, 403–418. doi: 10.1016/j.epsl.2007.01.030
- Crandell, D. R. (1989). *Gigantic Debris Avalanche of Pleistocene Age from Ancestral Mount Shasta Volcano, California, and Debris-Avalanche Hazard Zonation*. US: United States Geological Survey.
- Crisp, J. A. (1984). Rates of magma emplacement and volcanic output. *J. Volcanol. Geotherm. Res.* 20, 177–211. doi: 10.1016/0377-0273(84)90039-8
- Day, S., Llanes, P., Silver, E., Hoffmann, G., Ward, S., and Driscoll, N. (2015). Submarine landslide deposits of the historical lateral collapse of Ritter Island, Papua New Guinea. *Mar. Petrol. Geol.* 67, 419–438. doi: 10.1016/j.marpetgeo.2015.05.017
- de Saint Blanquat, M., Tikoff, B., Teyssier, C., and Vigneresse, J. L. (1998). Transpressional kinematics and magmatic arcs. *Geol. Soc. Lond. Spec. Publ.* 135, 327–340. doi: 10.1144/gsl.sp.1998.135.01.21
- del Potro, R., and Hürlimann, M. (2009). The decrease in the shear strength of volcanic materials with argillic hydrothermal alteration, insights from the summit region of Teide stratovolcano, Tenerife. *Eng. Geol.* 104, 135–143. doi: 10.1016/j.enggeo.2008.09.005

- Delcamp, A., de Vries, B. V. W., James, M. R., Gailler, L. S., and Lebas, E. (2012). Relationships between volcano gravitational spreading and magma intrusion. *Bull. Volcanol.* 74, 743–765. doi: 10.1007/s00445-011-0558-9
- Delcamp, A., Poppe, S., Detienne, M., and Paguican, E. M. R. (2018). “Destroying a volcanic edifice—interactions between edifice instabilities and the volcanic plumbing system,” in *Volcanic and Igneous Plumbing Systems*. Amsterdam, ed. S. Burchardt (Amsterdam: Elsevier), 231–257. doi: 10.1016/b978-0-12-809749-6.00009-1
- Delmelle, P., Henley, R. W., Opfergelt, S., and Detienne, M. (2015). “Summit acid crater lakes and flank instability in composite volcanoes,” in *Volcanic Lakes*, eds D. Rouwet, B. Christenson, F. Tassi, and J. Vandemeulebrouck (Berlin: Springer), 289–305. doi: 10.1007/978-3-642-36833-2_12
- Di Muro, A., Kueppers, U., Heap, M., Scharzlmüller, F., and Dingwell, D. (2021a). *From Permanent Flank Sliding to Catastrophic Collapse and Explosive Eruptions at Basaltic Volcanoes: the Role of Shallow Intrusive Magma Bodies*. Vienna: EGU General Assembly.
- Di Muro, A., Schwarzmüller, F., Kueppers, U., Heap, M., and Dingwell, D. (2021b). Petrophysical characterisation of volcanic ejecta to constrain subsurface lithological heterogeneities: implications for edifice stability at basaltic volcanoes. *Volcanica* 4, 41–66. doi: 10.30909/vol.04.01.4166
- Díaz, D., Zúñiga, F., and Castruccio, A. (2020). The interaction between active crustal faults and volcanism: a case study of the Liquiñe-Ofqui Fault Zone and Osorno volcano, southern Andes, using magnetotellurics. *J. Volcanol. Geotherm. Res.* 393:106806. doi: 10.1016/j.jvolgeores.2020.106806
- Dufresne, A., Zernack, A., Bernard, K., Thouret, J. C., and Roverato, M. (2021). “Sedimentology of volcanic debris avalanche deposits,” in *Volcanic Debris Avalanches: from Collapse to Hazard, Advances in Volcanology*, eds M. Roverato, A. Dufresne, and J. Procter (Berlin: Springer).
- Elsworth, D., and Day, S. J. (1999). Flank collapse triggered by intrusion: the Canarian and Cape Verde Archipelagos. *J. Volcanol. Geotherm. Res.* 94, 323–340. doi: 10.1016/s0377-0273(99)00110-9
- Elsworth, D., and Voight, B. (1995). Dike intrusion as a trigger for large earthquake and the failure of volcano flanks. *J. Geophys. Res. Solid Earth* 100, 6005–6024. doi: 10.1029/94jb02884
- Elsworth, D., and Voight, B. (1996). Evaluation of volcano flank instability triggered by dyke intrusion. *Geol. Soc. Spec. Publ.* 110, 45–53. doi: 10.1144/gsl.sp.1996.110.01.03
- Famin, V., and Michon, L. (2010). Volcano destabilization by magma injections in a detachment. *Geology* 38, 219–222. doi: 10.1130/g30717.1
- Farquharson, J. I., and Amelung, F. (2020). Extreme rainfall triggered the 2018 rift eruption at Kilauea volcano. *Nature* 580, 491–495. doi: 10.1038/s41586-020-2172-5
- Finizola, A., Sortino, F., Lénat, J. F., Aubert, M., Ripepe, M., and Valenza, M. (2003). The summit hydrothermal system of Stromboli. new insights from self-potential, temperature, CO₂ and fumarolic fluid measurements, with structural and monitoring implications. *Bull. Volcanol.* 65, 486–504. doi: 10.1007/s00445-003-0276-z
- Fox, J. M. (2019). *Complex Volcanic Architecture Produced by Basaltic Submarine and Emergent Volcanism in Intraplate Settings*. Doctoral dissertation. Australia: University of Tasmania.
- Francis, P., and Wells, A. (1988). LANDSAT thematic mapper observations of debris avalanche deposits in the Central Andes. *Bull. Volcanol.* 50, 258–278. doi: 10.1007/bf01047488
- Franco, L., Palma, J. L., Lara, L. E., Gil-Cruz, F., Cardona, C., Basualto, D., et al. (2019). Eruptive sequence and seismic activity of Llaima volcano (Chile) during the 2007–2009 eruptive period: inferences of the magmatic feeding system. *J. Volcanol. Geotherm. Res.* 379, 90–105. doi: 10.1016/j.jvolgeores.2019.04.014
- Giampiccolo, E., Cocina, O., De Gori, P., and Chiarabba, C. (2020). Dyke intrusion and stress-induced collapse of volcano flanks: the example of the 2018 event at Mt. Etna (Sicily, Italy). *Sci. Rep.* 10:6373.
- Giordano, D. (2019). Advances in the rheology of natural multiphase silicate melts: importance for magma transport and lava flow emplacement. *Ann. Geophys.* 62:VO216.
- Giordano, G., Porreca, M., Musacchio, P., and Mattei, M. (2008). The Holocene Secche di Lazzaro phreatomagmatic succession (Stromboli, Italy): evidence of pyroclastic density current origin deduced by facies analysis and AMS flow directions. *Bull. Volcanol.* 70, 1221–1236. doi: 10.1007/s00445-008-0198-x
- Glicken, H. (1991). *Sedimentary Architecture of Large Volcanic-debris Avalanches*. Tulsa: Society of Sedimentary Geologists.
- Glicken, H. (1996). *Rockslide-debris Avalanche of May 18, 1980, Mount St. Helens Volcano, Washington*. Washington, DC: United States Department of the Interior.
- Global Volcanism Program (2013). *Volcanoes of the World*, v. 4.9.4 (7 Mar 2021). Smithsonian Institution. Available online at: <https://doi.org/10.5479/si.GVP.VOTW4-2013> (accessed April 20, 2021).
- González, P. J., and Palano, M. (2014). Mt. Etna 2001 eruption: New insights into the magmatic feeding system and the mechanical response of the western flank from a detailed geodetic dataset. *J. Volcanol. Geotherm. Res.* 274, 108–121. doi: 10.1016/j.jvolgeores.2014.02.001
- Goto, Y., and Tomiya, A. (2019). Internal structures and growth style of a quaternary subaerial rhyodacite cryptodome at Ogariyama, Usu volcano, Hokkaido, Japan. *Front. Earth Sci.* 7:66.
- Gouhier, M., and Paris, R. (2019). SO₂ and tephra emissions during the December 22, 2018 Anak Krakatau flank-collapse eruption. *Volcanica* 2, 91–103. doi: 10.30909/vol.02.02.91103
- Greeley, R., and Spudis, P. D. (1981). Volcanism on mars. *Rev. Geophys.* 19, 13–41. doi: 10.1029/rg019i001p00013
- Gribble, R. F., Stern, R. J., Bloomer, S. H., Stüben, D., O’Hearn, T., and Newman, S. (1996). MORB mantle and subduction components interact to generate basalts in the southern mariana Trough back-arc basin. *Geochim. Cosmochim. Acta* 60, 2153–2166. doi: 10.1016/0016-7037(96)00078-6
- Grilli, S. T., Tappin, D. R., Carey, S., Watt, S. F., Ward, S. N., Grilli, A. R., et al. (2019). Modelling of the tsunami from the December 22, 2018 lateral collapse of Anak Krakatau volcano in the Sunda Straits, Indonesia. *Sci. Rep.* 9:11946.
- Gudmundsson, A. (2012). Magma chambers: formation, local stresses, excess pressures, and compartments. *J. Volcanol. Geotherm. Res.* 237, 19–41. doi: 10.1016/j.jvolgeores.2012.05.015
- Gudmundsson, A., Lecocq, N., Mohajeri, N., and Thordarson, T. (2014). Dike emplacement at Bardarbunga, Iceland, induces unusual stress changes, caldera deformation, and earthquakes. *Bull. Volcanol.* 76:869.
- Hacker, D. B., Rowley, P. D., and Biek, R. F. (2017). “Catastrophic collapse features in volcanic terrains: styles and links to subvolcanic magma systems,” in *Physical Geology of Shallow Magmatic Systems*, eds C. Breitkreuz and S. Rocchi (Cham: Springer), 215–248. doi: 10.1007/978-3-319-14084-1_1001
- Harp, A. G., and Valentine, G. A. (2018). Emplacement controls for the basaltic-andesitic radial dikes of summer con volcano and implications for flank vents at stratovolcanoes. *Bull. Volcanol.* 80:16.
- Head, J. W., and McCord, T. B. (1978). Imbrian-age highland volcanism on the moon: the Gruithuisen and Mairan domes. *Science* 199, 1433–1436. doi: 10.1126/science.199.4336.1433
- Head, J. W., Chapman, C. R., Strom, R. G., Fassett, C. I., Denevi, B. W., Blewett, D. T., et al. (2011). Flood volcanism in the northern high latitudes of mercury revealed by messenger. *Science* 333, 1853–1856. doi: 10.1126/science.1211997
- Head, J. W., Crumpler, L. S., Aubele, J. C., Guest, J. E., and Saunders, R. S. (1992). Venus volcanism: classification of volcanic features and structures, associations, and global distribution from Magellan data. *J. Geophys. Res. Planets* 97, 13153–13197. doi: 10.1029/92je01273
- Head, J. W., Murchie, S. L., Prockter, L. M., Robinson, M. S., Solomon, S. C., Strom, R. G., et al. (2008). Volcanism on mercury: evidence from the first messenger flyby. *Science* 321, 69–72. doi: 10.1126/science.1159256
- Hickey, J., Lloyd, R., Biggs, J., Arnold, D., Mothes, P., and Muller, C. (2020). Rapid localized flank inflation and implications for potential slope instability at Tungurahua volcano, Ecuador. *Earth Planet. Sci. Lett.* 534:116104. doi: 10.1016/j.epsl.2020.116104
- Hildreth, W., Singer, B., Godoy, E., and Munizaga, F. (1998). The age and constitution of Cerro Campanario, a mafic stratovolcano in the andes of central Chile. *Rev. Geol. Chile* 25, 17–28.
- Houghton, B. F., and Gonnermann, H. M. (2008). Basaltic explosive volcanism: constraints from deposits and models. *Geochemistry* 68, 117–140. doi: 10.1016/j.jchemer.2008.04.002
- Intrieri, E., Di Traglia, F., Del Ventisette, C., Gigli, G., Mugnai, F., Luzi, G., et al. (2013). Flank instability of Stromboli volcano (Aeolian Islands, Southern Italy):

- integration of GB-InSAR and geomorphological observations. *Geomorphology* 201, 60–69. doi: 10.1016/j.geomorph.2013.06.007
- Jerram, D. A., and Bryan, S. E. (2015). “Plumbing systems of shallow level intrusive complexes,” in *Physical Geology of Shallow Magmatic Systems*, eds C. Bretkreuz and S. Rocchi (Cham: Springer), 39–60. doi: 10.1007/978-3-319-14084-1_8
- Jicha, B. R., Laabs, B. J., Hora, J. M., Singer, B. S., and Caffee, M. W. (2015). Early Holocene collapse of Volcán Paríacota, central Andes, Chile: volcanological and paleohydrological consequences. *Geol. Soc. Am. Bull.* 127, 1681–1688. doi: 10.1130/b31247.1
- Karstens, J., Berndt, C., Urlaub, M., Watt, S. F., Micallef, A., Ray, M., et al. (2019). From gradual spreading to catastrophic collapse—reconstruction of the 1888 Ritter Island volcanic sector collapse from high-resolution 3D seismic data. *Earth Planet. Sci. Lett.* 517, 1–13. doi: 10.1016/j.epsl.2019.04.009
- Keating, B. H., and McGuire, W. J. (2004). Instability and structural failure at volcanic ocean islands and the climate change dimension. *Adv. Geophys.* 47, 175–271. doi: 10.1016/s0065-2687(04)47004-6
- Keating, G. N., Valentine, G. A., Krier, D. J., and Perry, F. V. (2008). Shallow plumbing systems for small-volume basaltic volcanoes. *Bull. Volcanol.* 70, 563–582. doi: 10.1007/s00445-007-0154-1
- Keefer, D. K. (2002). Investigating landslides caused by earthquakes—a historical review. *Surv. Geophys.* 23, 473–510.
- Kendrick, J. E., Smith, R., Sammonds, P., Meredith, P. G., Dainty, M., and Pallister, J. D. (2013). The influence of thermal and cyclic stressing on the strength of rock from Mount St. Helens, Washington. *Bull. Volcanol.* 75:728.
- Kereszturi, G., and Németh, K. (2012). “Monogenetic basaltic volcanoes: genetic classification, growth, geomorphology and degradation,” in *Updates in Volcanology—New Advances in Understanding Volcanic Systems*, ed. K. Németh (Germany: BoD – Books on Demand).
- Kerle, N., de Vries, B. V. W., and Oppenheimer, C. (2003). New insight into the factors leading to the 1998 flank collapse and lahar disaster at Casita volcano, Nicaragua. *Bull. Volcanol.* 65, 331–345. doi: 10.1007/s00445-002-0263-9
- Kitamura, S., and Matías, O. (1995). Tephra stratigraphic approach to the eruptive history of Pacaya volcano, Guatemala. *Sci. Rep. Tohoku Univ. Seventh Ser. Geogr.* 45, 1–41.
- Kristmannsdóttir, H. (1979). “Alteration of basaltic rocks by hydrothermal-activity at 100–300 °C,” in *Developments in Sedimentology*, eds M. Rebesco and A. Camerlenghi (Amsterdam: Elsevier).
- Kushendratno, Pallister, J. S., Bina, F. R., McCausland, W., Carn, S., Haerani, N., et al. (2012). Recent explosive eruptions and volcano hazards at Soputan volcano—a basalt stratovolcano in north Sulawesi, Indonesia. *Bull. Volcanol.* 74, 1581–1609. doi: 10.1007/s00445-012-0620-2
- Lagmay, A. M. F., De Vries, B. V. W., Kerle, N., and Pyle, D. M. (2000). Volcano instability induced by strike-slip faulting. *Bull. Volcanol.* 62, 331–346. doi: 10.1007/s004450000103
- Landi, P., Francalanci, L., Pompilio, M., Rosi, M., Corsaro, R. A., Petrone, C. M., et al. (2006). The December 2002–July 2003 effusive event at Stromboli volcano, Italy: insights into the shallow plumbing system by petrochemical studies. *J. Volcanol. Geotherm. Res.* 155, 263–284. doi: 10.1016/j.jvolgeores.2006.03.032
- Lastras, G., Amblas, D., Calafat, A. M., Canals, M., Frigola, J., Hermanns, R. L., et al. (2013). Landslides cause tsunami waves: insights from Aysén fjord, Chile. *Eos Trans. Am. Geophys. Union* 94, 297–298. doi: 10.1002/2013eo340002
- Leshner, C. E., and Spera, F. J. (2015). “Thermodynamic and transport properties of silicate melts and magma,” in *The Encyclopedia of Volcanoes*, eds H. Sigurdsson, B. Houghton, S. McNutt, H. Rymer, and J. Stix (Amsterdam: Elsevier).
- Leyrit, H. (2000). “Flank collapse and debris avalanche deposits,” in *Volcaniclastic Rocks, from Magmas to Sediments*, eds H. Leyrit and C. Montenat (Boca Raton, FL: CRC Press), 111–129.
- Lindoo, A., Larsen, J. F., Cashman, K. V., and Oppenheimer, J. (2017). Crystal controls on permeability development and degassing in basaltic andesite magma. *Geology* 45, 831–834. doi: 10.1130/g39157.1
- Liotta, M., Paonita, A., Caracausi, A., Martelli, M., Rizzo, A., and Favara, R. (2010). Hydrothermal processes governing the geochemistry of the crater fumaroles at Mount Etna volcano (Italy). *Chem. Geol.* 278, 92–104. doi: 10.1016/j.chemgeo.2010.09.004
- Liu, C., Lay, T., and Xiong, X. (2018). Rupture in the 4 May 2018 MW 6.9 earthquake seaward of the Kilauea east rift zone fissure eruption in Hawaii. *Geophys. Res. Lett.* 45, 9508–9515. doi: 10.1029/2018gl079349
- Lohmar, S. (2000). *Estratigrafía, Petrografía y Geoquímica del Volcán Antuco y sus Depósitos (Andes del Sur, 37°25'S)*. *Memoria de Título (Unpublished)*. Chile: Universidad de Concepción.
- Lundgren, P., Casu, F., Manzo, M., Pepe, A., Berardino, P., Sansosti, E., et al. (2004). Gravity and magma induced spreading of Mount Etna volcano revealed by satellite radar interferometry. *Geophys. Res. Lett.* 31, L04602–L04606.
- Maccaferri, F., Richter, N., and Walter, T. R. (2017). The effect of giant lateral collapses on magma pathways and the location of volcanism. *Nat. Commun.* 8:1097.
- Malone, S., Weaver, C., and Endo, E. (1981). *Seismic Details of the May 18, 1980 Cataclysmic Eruption of Mount St. Helens*. US: United States Geological Survey.
- Manconi, A., Longpré, M. A., Walter, T. R., Troll, V. R., and Hansteen, T. H. (2009). The effects of flank collapses on volcano plumbing systems. *Geology* 37, 1099–1102. doi: 10.1130/g30104a.1
- Marinos, P., and Hoek, E. (2000). “GSI—a geologically friendly tool for rockmass strength estimation,” in *Proceedings of the GeoEng 2000 Conference*, (Melbourne).
- Martínez, P., Singer, B. S., Roa, H. M., and Jicha, B. R. (2018). Volcanologic and petrologic evolution of Antuco-Sierra Velluda, Southern Andes, Chile. *J. Volcanol. Geotherm. Res.* 349, 392–408. doi: 10.1016/j.jvolgeores.2017.11.026
- Masson, D. G., Watts, A. B., Gee, M. J. R., Urgeles, R., Mitchell, N. C., Le Bas, T. P., et al. (2002). Slope failures on the flanks of the western Canary Islands. *Earth Sci. Rev.* 57, 1–35. doi: 10.1016/s0012-8252(01)00069-1
- Mathieu, L., van Wyk de Vries, B., Pilato, M., and Troll, V. R. (2011). The interaction between volcanoes and strike-slip, transtensional and transpressional fault zones: analogue models and natural examples. *J. Struct. Geol.* 33, 898–906. doi: 10.1016/j.jsg.2011.03.003
- McGuire, W. J. (1996). Volcano instability: a review of contemporary themes. *Geol. Soc. Spec. Publ.* 110, 1–23. doi: 10.1144/gsl.sp.1996.110.01.01
- McGuire, W. J. (2006). Lateral collapse and tsunamigenic potential of marine volcanoes. *Geol. Soc. Lond. Spec. Publ.* 269, 121–140. doi: 10.1144/gsl.sp.2006.269.01.08
- McPhail, D. D. (1973). The geomorphology of the rio Teno lahar, central Chile. *Geogr. Rev.* 63, 517–532. doi: 10.2307/213919
- Merle, O., and Borgia, A. (1996). Scaled experiments of volcanic spreading. *J. Geophys. Res. Solid Earth* 101, 13805–13817. doi: 10.1029/95jb03736
- Miraglia, L. (2006). The December 2002–July 2003 effusive event at Stromboli volcano, Italy: insights into the shallow plumbing system by petrochemical studies. *J. Volcanol. Geotherm. Res.* 155, 263–284. doi: 10.1016/j.jvolgeores.2006.03.032
- Miyaji, N., Togashi, S., and Chiba, T. (2004). A large-scale collapse event at the eastern slope of Fuji volcano about 2900 years ago. *Bull. Volcanol. Soc. Japan* 49, 237–248.
- Montanaro, C., Beget, J., Marti, J., Siebert, L., and Coombs, M. (2011). Volcano collapse along the Aleutian Ridge (western Aleutian Arc). *Nat. Haz. Earth Syst. Sci.* 11, 715–730. doi: 10.5194/nhess-11-715-2011
- Monzier, M., Robin, C., Samaniego, P., Hall, M. L., Cotten, J., Mothes, P., et al. (1999). Sangay volcano, Ecuador: structural development, present activity and petrology. *J. Volcanol. Geotherm. Res.* 90, 49–79. doi: 10.1016/s0377-0273(99)00021-9
- Moon, V., and Jayawardane, J. (2004). Geomechanical and geochemical changes during early stages of weathering of Karamu Basalt, New Zealand. *Eng. Geol.* 74, 57–72. doi: 10.1016/j.enggeo.2004.02.002
- Moreno, H., Lohmar, S., López-Escobar, L., and Petit-Breuilh, M. E. (2000). “Contribución a la evolución geológica, geoquímica e impacto ambiental del Volcán Antuco (Andes del Sur, 37° 25'S),” in *Proceedings of Thre IX Congreso Geológico Chileno*, (Chile).
- Moriya, I. (1980). *Bandaian Eruption and Landforms Associated with it*. Collection of Articles in Memory of Retirement of Prof. K. Nishimura from Tohoku University. Fac. Sci. Sendai: Tohoku University, 214–219.
- Münn, S., Walter, T. R., and Klügel, A. (2006). Gravitational spreading controls rift zones and flank instability on El Hierro, Canary Islands. *Geol. Mag.* 143, 257–268. doi: 10.1017/s0016756806002019

- Naranjo, J. A., and Haller, M. J. (2002). Erupciones holocenas principalmente explosivas del volcán Planchón, Andes del sur (35° 15'S). *Revista Geológica de Chile* 29, 93–113.
- Naranjo, J. A., Haller, M. J., Ostera, H. A., Pesce, A. H., and Sruoga, P. (1999). *Geología y peligros del Complejo Volcánico Planchón-Peteroa, Andes del Sur (35° 15'S), Región del Maule, Chile-Provincia de Mendoza, Argentina*. Santiago: Servicio Nacional de Geología y Minería, Boletín.
- Natland, J. H., and Atlas, Z. (2003). Massive pyroclastic eruptions accompanied the sector collapse of Oahu and the Nuuanu Landslide: petrological evidence for a submarine directed blast. *AGUFM* 2003, 12B–0453B.
- Navarre-Sitchler, A., Steefel, C. I., Yang, L., Tomutsa, L., and Brantley, S. L. (2009). Evolution of porosity and diffusivity associated with chemical weathering of a basalt clast. *J. Geophys. Res. Earth Surface* 114:F02016.
- Németh, K., and Kereszturi, G. (2015). Monogenetic volcanism: personal views and discussion. *Int. J. Earth Sci.* 104, 2131–2146. doi: 10.1007/s00531-015-1243-6
- Németh, K., Risso, C., Nullo, F., and Kereszturi, G. (2011). The role of collapsing and cone rafting on eruption style changes and final cone morphology: Los Morados scoria cone, Mendoza, Argentina. *Central Eur. J. Geosci.* 3, 102–118.
- Nolesini, T., Di Traglia, F., Del Ventisette, C., Moretti, S., and Casagli, N. (2013). Deformations and slope instability on Stromboli volcano: integration of GBInSAR data and analog modeling. *Geomorphology* 180, 242–254. doi: 10.1016/j.geomorph.2012.10.014
- Norini, G., and Acocella, V. (2011). Analogue modeling of flank instability at Mount Etna: understanding the driving factors. *J. Geophys. Res. Solid Earth* 116, B07206.
- Norini, G., Bustos, E., Arnoso, M., Baez, W., Zuluaga, M. C., and Roverato, M. (2020). Unusual volcanic instability and sector collapse configuration at Chimpa volcano, central Andes. *J. Volcanol. Geotherm. Res.* 393:106808.
- Oehler, J. F., de Vries, B. V. W., and Labazuy, P. (2005). Landslides and spreading of oceanic hot-spot and arc shield volcanoes on Low Strength layers (LSLs): an analogue modeling approach. *J. Volcanol. Geotherm. Res.* 144, 169–189. doi: 10.1016/j.jvolgeores.2004.11.023
- Oehler, J. F., Lénat, J. F., and Labazuy, P. (2008). Growth and collapse of the reunion Island volcanoes. *Bull. Volcanol.* 70, 717–742. doi: 10.1007/s00445-007-0163-0
- Ortiz, R., Moreno, H., García, A., Fuentealba, G., Astiz, M., Peña, P., et al. (2003). Villarrica volcano (Chile): characteristics of the volcanic tremor and forecasting of small explosions by means of a material failure method. *J. Volcanol. Geotherm. Res.* 128, 247–259. doi: 10.1016/s0377-0273(03)00258-0
- Paguican, E. M. R., van Wyk, de Vries, B., and Lagmay, A. M. F. (2012). Volcano-tectonic controls and emplacement kinematics of the Iriga debris avalanches (Philippines). *Bull. Volcanol.* 74, 2067–2081. doi: 10.1007/s00445-012-0652-7
- Pallister, J. S., Bina, F. R., McCausland, W., Carn, S., Haerani, N., Griswold, J., et al. (2012). Recent explosive eruptions and volcano hazards at Soputan volcano—a basalt stratovolcano in north Sulawesi. *Indonesia. Bull. Volcanol.* 74, 1581–1609. doi: 10.1007/s00445-012-0620-2
- Palmer, B. A., Alloway, B. V., and Neall, V. E. (1991). “Volcanic debris avalanche deposits in New Zealand—lithofacies organization in unconfined, wet-avalanche flows,” in *Sedimentation in Volcanic Settings*, eds R. V. Fisher and G. A. Smith (Tulsa: Society of Sedimentary Geologists).
- Pearce, R. K., Sánchez de la Muela, A., Moorkamp, M., Hammond, J. O., Mitchell, T. M., Cembrano, J., et al. (2020). Reactivation of fault systems by compartmentalized hydrothermal fluids in the Southern Andes revealed by magnetotelluric and seismic data. *Tectonics* 39:e2019TC005997.
- Pérez-Flores, P., Cembrano, J., Sánchez-Alfaro, P., Veloso, E., Arancibia, G., and Roquer, T. (2016). Tectonics, magmatism and paleo-fluid distribution in a strike-slip setting: insights from the northern termination of the Liquiñe-Ofqui fault System. *Chile. Tectonophys.* 680, 192–210. doi: 10.1016/j.tecto.2016.05.016
- Petrone, C. M., Braschi, E., and Francalanci, L. (2009). Understanding the collapse-eruption link at Stromboli, Italy: a microanalytical study on the products of the recent Secche di Lazzaro phreatomagmatic activity. *J. Volcanol. Geotherm. Res.* 188, 315–332. doi: 10.1016/j.jvolgeores.2009.09.016
- Pichavant, M., Di Carlo, I., Rotolo, S. G., Scaillet, B., Burgisser, A., Le Gall, N., et al. (2013). Generation of CO₂-rich melts during basalt magma ascent and degassing. *Contrib. Mineral. Petrol.* 166, 545–561. doi: 10.1007/s00410-013-0890-5
- Pinel, V., and Albino, F. (2013). Consequences of volcano sector collapse on magmatic storage zones: insights from numerical modeling. *J. Volcanol. Geotherm. Res.* 252, 29–37. doi: 10.1016/j.jvolgeores.2012.11.009
- Pinel, V., and Jaupart, C. (2005). Some consequences of volcanic edifice destruction for eruption conditions. *J. Volcanol. Geotherm. Res.* 145, 68–80. doi: 10.1016/j.jvolgeores.2005.01.012
- Piquer, J., Yáñez, G., Rivera, O., and Cooke, D. R. (2019). Long-lived crustal damage zones associated with fault intersections in the high Andes of central Chile. *Andean Geol.* 46, 223–239. doi: 10.5027/andgeov46n2-3106
- Polá, A., Crosta, G. B., Fusi, N., and Castellanza, R. (2014). General characterization of the mechanical behaviour of different volcanic rocks with respect to alteration. *Eng. Geol.* 169, 1–13. doi: 10.1016/j.enggeo.2013.11.011
- Polanco, E., and Naranjo, J. A. (2008). “Colapso holoceno en el volcán callaqui (37°55'S), Andes del Sur,” in *Proceedings of the XVII Congreso Geológico Argentino*, (Jujuy), 1157–1158.
- Poland, M. P., Peltier, A., Bonforte, A., and Puglisi, G. (2017). The spectrum of persistent volcanic flank instability: a review and proposed framework based on Kilauea, Piton de la Fournaise, and Etna. *J. Volcanol. Geotherm. Res.* 339, 63–80. doi: 10.1016/j.jvolgeores.2017.05.004
- Ponomareva, V. V., Melekestsev, I. V., and Dirksen, O. V. (2006). Sector collapses and large landslides on late pleistocene–holocene volcanoes in kamchatka, Russia. *J. Volcanol. Geotherm. Res.* 158, 117–138. doi: 10.1016/j.jvolgeores.2006.04.016
- Quidelleur, X., Hildenbrand, A., and Samper, A. (2008). Causal link between Quaternary paleoclimatic changes and volcanic islands evolution. *Geophys. Res. Lett.* 35:L02303. doi: 10.1029/2007GL031849
- Reid, M. E., Keith, T. E., Kayen, R. E., Iverson, N. R., Iverson, R. M., and Brien, D. L. (2010). Volcano collapse promoted by progressive strength reduction: new data from Mount St. Helens. *Bull. Volcanol.* 72, 761–766. doi: 10.1007/s00445-010-0377-4
- Roberti, G., Roberts, N. J., and Lit, C. (2021). “Climatic influence on volcanic landslides,” in *Volcanic Debris Avalanches: from Collapse to Hazard. Advances in Volcanology*, eds M. Roverato, A. Dufresne, and J. Procter (Berlin: Springer).
- Rodríguez, A., and van Bergen, M. J. (2017). Superficial alteration mineralogy in active volcanic systems: an example of Poás volcano, Costa Rica. *J. Volcanol. Geotherm. Res.* 346, 54–80. doi: 10.1016/j.jvolgeores.2017.04.006
- Romero, C., Galindo, I., Sánchez, N., Martín-González, E., and Vegas, J. (2020a). “Syn-eruptive lateral collapse of monogenetic volcanoes: the case of mazo volcano from the timanfaya eruption (Lanzarote, Canary Islands),” in *Volcanoes-Updates in Volcanology*, ed. K. Nemeth (Germany: BoD – Books on Demand).
- Romero, J. E., Aguilera, F., Delgado, F., Guzmán, D., Van Eaton, A. R., Luengo, N., et al. (2020b). Combining ash analyses with remote sensing to identify juvenile magma involvement and fragmentation mechanisms during the 2018/19 small eruption of Peteroa volcano (Southern Andes). *J. Volcanol. Geotherm. Res.* 402:106984. doi: 10.1016/j.jvolgeores.2020.106984
- Romero, J. E., Ramírez, V., Alam, M. A., Bustillos, J., Guevara, A., Urrutia, R., et al. (2020c). Pyroclastic deposits and eruptive heterogeneity of Volcán Antuco (37° S; Southern Andes) during the Mid to Late Holocene (< 7.2 ka). *J. Volcanol. Geotherm. Res.* 392:106759. doi: 10.1016/j.jvolgeores.2019.106759
- Romero, J., Keller Ulrich, W., and Marfull, V. (2013). Short chronological analysis of the 2007–2009 eruptive cycle and its nested cones formation at Llaima volcano. *J. Technol. Possibilism* 2, 1–9. doi: 10.1016/j.jvolgeores.2011.05.003
- Romero, J., Polacci, M., Moreno, H., Watt, S., Parada, M. A., Valenzuela, K., et al. (2021). “Multi-scale impacts of Antuco basaltic stratovolcano (Southern Andes, Chile) ca. 6.2 ka sector collapse: avalanche deposition, eruptive behavior transformation and hydrologic reconfiguration,” in *Proceedings of the EGU General Assembly*, (Austria).
- Rose, W. I., Palma, J. L., Escobar Wolf, R., and Matías, R. O. (2010). *A 50 yr Eruption of a Basaltic Composite Cone: Pacaya, Guatemala*. Boulder, Co: Geological Society of America.
- Roverato, M., Capra, L., Sulpizio, R., and Norini, G. (2011). Stratigraphic reconstruction of two debris avalanche deposits at Colima Volcano (Mexico): insights into pre-failure conditions and climate influence. *J. Volcanol. Geotherm. Res.* 207, 33–46. doi: 10.1016/j.jvolgeores.2011.07.003
- Roverato, M., Cronin, S., Procter, J., and Capra, L. (2015). Textural features as indicators of debris avalanche transport and emplacement. *Taranaki Volcano GSA Bull.* 127, 3–18. doi: 10.1130/b30946.1
- Roverato, M., Di Traglia, F., Procter, J., Paguican, E. M. R., and Dufresne, A. (2021). “Factors contributing to volcano lateral collapse,” in *Volcanic Debris Avalanches:*

- from Collapse to Hazard, eds M. Roverato, A. Dufresne, and J. Procter (Berlin: Springer).
- Sassa, K., Dang, K., Yanagisawa, H., and He, B. (2016). A new landslide-induced tsunami simulation model and its application to the 1792 Unzen-Mayuyama landslide-and-tsunami disaster. *Landslides* 13, 1405–1419. doi: 10.1007/s10346-016-0691-9
- Satake, K. (2007). Volcanic origin of the 1741 Oshima-Oshima tsunami in the Japan sea. *Earth Planets Space* 59, 381–390. doi: 10.1186/bf03352698
- Satake, K., and Kato, Y. (2001). The 1741 Oshima-Oshima eruption: extent and volume of submarine debris avalanche. *Geophys. Res. Lett.* 28, 427–430. doi: 10.1029/2000gl012175
- Schaefer, L. N., Di Traglia, F., Chaussard, E., Lu, Z., Nolesini, T., and Casagli, N. (2019). Monitoring volcano slope instability with synthetic aperture radar: a review and new data from Pacaya (Guatemala) and Stromboli (Italy) volcanoes. *Earth Sci. Rev.* 192, 236–257. doi: 10.1016/j.earscirev.2019.03.009
- Schaefer, L. N., Kendrick, J. E., Oommen, T., Lavallée, Y., and Chigna, G. (2015). Geomechanical rock properties of a basaltic volcano. *Front. Earth Sci.* 3:29.
- Schaefer, L. N., Oommen, T., Corazzato, C., Tibaldi, A., Escobar-Wolf, R., and Rose, W. I. (2013). An integrated field-numerical approach to assess slope stability hazards at volcanoes: the example of Pacaya, Guatemala. *Bull. Volcanol.* 75:720.
- Schmidt, M. W., and Poli, S. (1998). Experimentally based water budgets for dehydrating slabs and consequences for arc magma generation. *Earth Planet. Sci. Lett.* 163, 361–379. doi: 10.1016/s0012-821x(98)00142-3
- Schön, J. H. (2015). *Physical Properties of Rocks: Fundamentals and Principles of Petrophysics*. Amsterdam: Elsevier.
- Scott, K. M., Macías, J. L., Naranjo, J. A., Rodríguez, S., and McGeehin, J. P. (2001). *Catastrophic Debris Flows Transformed from Landslides in Volcanic Terrains: Mobility, Hazard Assessment, and Mitigation Strategies (No. 1630)*. US: US Geological Survey.
- Scott, K. M., Vallance, J. W., and Pringle, P. T. (1995). *Sedimentology, Behavior, and Hazards of Debris Flows at Mount Rainier, Washington*. US: US Geological Survey.
- Scott, K. M., Vallance, J. W., Kerle, N., Luis Macías, J., Strauch, W., and Devoli, G. (2005). Catastrophic precipitation-triggered lahar at Casita volcano, Nicaragua: occurrence, bulking and transformation. *Earth Surface Process. Landf.* 30, 59–79. doi: 10.1002/esp.1127
- Sepúlveda, S. A., Serey, A., Lara, M., Pavez, A., and Rebolledo, S. (2010). Landslides induced by the April 2007 Aysén fjord earthquake, Chilean Patagonia. *Landslides* 7, 483–492. doi: 10.1007/s10346-010-0203-2
- Shea, T., and Hammer, J. E. (2013). Kinetics of cooling-and decompression-induced crystallization in hydrous mafic-intermediate magmas. *J. Volcanol. Geotherm. Res.* 260, 127–145. doi: 10.1016/j.jvolgeores.2013.04.018
- Sheth, H. C. (1999). Flood basalts and large igneous provinces from deep mantle plumes: fact, fiction, and fallacy. *Tectonophysics* 311, 1–29. doi: 10.1016/s0040-1951(99)00150-x
- Sheth, H. C., Ray, J. S., Bhutani, R., Kumar, A., and Smitha, R. S. (2009). Volcanology and eruptive styles of Barren Island: an active mafic stratovolcano in the Andaman Sea, NE Indian Ocean. *Bull. Volcanol.* 71:1021. doi: 10.1007/s00445-009-0280-z
- Siebert, L. (1984). Large volcanic debris avalanches: characteristics of source areas, deposits, and associated eruptions. *J. Volcanol. Geotherm. Res.* 22, 163–197. doi: 10.1016/0377-0273(84)90002-7
- Siebert, L. (2002). “Landslides resulting from structural failure of volcanoes” in *Catastrophic Landslides: Effects, Occurrence, and Mechanisms*, eds S. G. Evans and J. V. DeGraff (Boulder, CO: Geological Society of America).
- Siebert, L., and Roverato, M. (2021). “A historical perspective on lateral collapse and debris avalanches,” in *Volcanic Debris Avalanches: from Collapse to Hazard, Advances in Volcanology*, eds M. Roverato, A. Dufresne, and J. Procter (Berlin: Springer).
- Sielfeld, G., Cembrano, J., and Lara, L. (2017). Transtension driving volcano-edifice anatomy: insights from Andean transverse-to-the-orogen tectonic domains. *Quat. Int.* 438, 33–49. doi: 10.1016/j.quaint.2016.01.002
- Sielfeld, G., Ruz, J., Brogi, A., Cembrano, J., Stanton-Yonge, A., Pérez-Flores, P., et al. (2019). Oblique-slip tectonics in an active volcanic chain: a case study from the Southern Andes. *Tectonophysics* 770:228221. doi: 10.1016/j.tecto.2019.228221
- Skjelkvåle, B. L., Amundsen, H. E. F., O'Reilly, S. Y., Griffin, W. L., and Gjelsvik, T. (1989). A primitive alkali basaltic stratovolcano and associated eruptive centres, northwestern Spitsbergen: volcanology and tectonic significance. *J. Volcanol. Geotherm. Res.* 37, 1–19. doi: 10.1016/0377-0273(89)90110-8
- Solaro, G., Acocella, V., Pepe, S., Ruch, J., Neri, M., and Sansosti, E. (2010). Anatomy of an unstable volcano from InSAR: multiple processes affecting flank instability at Mt. Etna, 1994–2008. *J. Geophys. Res. Solid Earth* 115:B10405. doi: 10.1029/2009JB008020
- Stern, C., Moreno, H., López-Escobar, L., Clavero, J. E., Lara, L. E., Naranjo, J. A., et al. (2007). “Chilean volcanoes,” in *The Geology of Chile*, eds T. Moreno and W. Gibbons (The Geological Society: London), 21–114.
- Strom, R. G., Trask, N. J., and Guest, J. E. (1975). Tectonism and volcanism on mercury. *J. Geophys. Res.* 80, 2478–2507. doi: 10.1029/jb080i017p02478
- Tibaldi, A. (1995). Morphology of pyroclastic cones and tectonics. *J. Geophys. Res. Solid Earth* 100, 24521–24535. doi: 10.1029/95jb02250
- Tibaldi, A. (2004). Major changes in volcano behaviour after a sector collapse: insights from Stromboli, Italy. *Terra Nova* 16, 2–8. doi: 10.1046/j.1365-3121.2003.00517.x
- Tibaldi, A., Corazzato, C., Kozhurin, A., Lagmay, A. F., Pasquare, F. A., Ponomareva, V. V., et al. (2008). Influence of substrate tectonic heritage on the evolution of composite volcanoes: predicting sites of flank eruption, lateral collapse, and erosion. *Glob. Planet. Change* 61, 151–174. doi: 10.1016/j.gloplacha.2007.08.014
- Tibaldi, A., Pasquare, F., and Tormey, D. (2009). “Volcanism in reverse and strike-slip fault settings,” in *New Frontiers in Integrated Solid Earth Sciences*, eds S. Cloetingh and J. Negendank (Dordrecht: Springer), 315–348. doi: 10.1007/978-90-481-2737-5_9
- Tinti, S., Manucci, A., Pagnoni, G., Armigliato, A., and Zaniboni, F. (2005). The 30 December 2002 landslide-induced tsunamis in Stromboli: sequence of the events reconstructed from the eyewitness accounts. *Nat. Haz. Earth Syst. Sci.* 5, 763–775. doi: 10.5194/nhess-5-763-2005
- Tormey, D. (2010). Managing the effects of accelerated glacial melting on volcanic collapse and debris flows: Planchon–Petroa Volcano, Southern Andes. *Global Planet. Change* 74, 82–90. doi: 10.1016/j.gloplacha.2010.08.003
- Tormey, D. R., Frey, F. A., and Lopez-Escobar, L. (1995). Geochemistry of the active Azufre-Planchon-Petroa volcanic complex, Chile (35° 15' S): evidence for multiple sources and processes in a cordilleran arc magmatic system. *J. Petrol.* 36, 265–298. doi: 10.1093/petrology/36.2.265
- Tost, M., and Cronin, S. J. (2016). Climate influence on volcano edifice stability and fluvial landscape evolution surrounding Mount Ruapehu, New Zealand. *Geomorphology* 262, 77–90. doi: 10.1016/j.geomorph.2016.03.017
- Tost, M., Cronin, S. J., Procter, J. N., Smith, I. E. M., Neall, V. E., and Price, R. C. (2015). Impacts of catastrophic volcanic collapse on the erosion and morphology of a distal fluvial landscape: Hautapu river, Mount Ruapehu, New Zealand. *Geol. Soc. Am. Bull.* 127, 266–280. doi: 10.1130/b31010.1
- Ui, T. (1983). Volcanic dry avalanche deposits—identification and comparison with nonvolcanic debris stream deposits. *J. Volcanol. Geotherm. Res.* 18, 135–150. doi: 10.1016/0377-0273(83)90006-9
- Ui, T. (1989). “Discrimination between debris avalanches and other volcanoclastic deposits,” in *Volcanic Hazards. IAVCEI Proceedings in Volcanology*, Vol. 1, ed J. H. Latter (Berlin: Springer), 201–209. doi: 10.1007/978-3-642-73759-6_13
- Valentine, G. A., and Connor, C. B. (2015). “Basaltic volcanic fields,” in *The Encyclopedia of Volcanoes*, eds H. Sigurdsson, B. Houghton, S. McNutt, H. Rymer, and J. Stix (Amsterdam: Elsevier).
- Valentine, G. A., and Gregg, T. K. P. (2008). Continental basaltic volcanoes—processes and problems. *J. Volcanol. Geotherm. Res.* 177, 857–873. doi: 10.1016/j.jvolgeores.2008.01.050
- Valentine, G. A., Cortés, J. A., Widom, E., Smith, E. I., Rasoanamparany, C., Johnsen, R., et al. (2017). Lunar crater volcanic field (reveille and pancake ranges, basin and Range Province, Nevada, USA). *Geosphere* 13, 391–438. doi: 10.1130/ges01428.1
- Valentine, G. A., Perry, F. V., Krier, D., Keating, G. N., Kelley, R. E., and Cogbill, A. H. (2006). Small-volume basaltic volcanoes: eruptive products and processes, and post-eruptive geomorphic evolution in Crater Flat (Pleistocene), southern Nevada. *Geol. Soc. Am. Bull.* 118, 1313–1330. doi: 10.1130/b25956.1
- Vallance, J. W., and Scott, K. M. (1997). The Osceola Mudflow from Mount Rainier: sedimentology and hazard implications of a huge clay-rich debris flow. *Geol.*

- Soc. Am. Bull. 109, 143–163. doi: 10.1130/0016-7606(1997)109<0143:tomfmr>2.3.co;2
- Vallance, J. W., Siebert, L., Rose, W. I., Girón, J. R., and Banks, N. G. (1995). Edifice collapse and related hazards in Guatemala. *J. Volcanol. Geotherm. Res.* 66, 337–355. doi: 10.1016/0377-0273(94)00076-s
- Valverde, V., Mothes, P. A., Beate, B., and Bernard, J. (2021). Enormous and far-reaching debris avalanche deposits from Sangay volcano (Ecuador): multidisciplinary study and modeling the 30 ka sector collapse. *J. Volcanol. Geotherm. Res.* 411:107172. doi: 10.1016/j.jvolgeores.2021.107172
- van Daele, M., Moernaut, J., Silversmit, G., Schmidt, S., Fontijn, K., Heirman, K., et al. (2014). The 600 yr eruptive history of Villarrica Volcano (Chile) revealed by annually laminated lake sediments. *Bulletin* 126, 481–498. doi: 10.1130/b30798.1
- van Wyk de Vries, B., and Davies, T. (2015). “Chapter 38 – landslides, debris avalanches, and volcanic gravitational deformation,” in *The Encyclopedia of Volcanoes*, eds H. Sigurdsson, B. Houghton, S. McNutt, H. Rymer, and J. Stix (Amsterdam: Elsevier).
- van Wyk de Vries, B., and Francis, P. W. (1997). Catastrophic collapse at stratovolcanoes induced by gradual volcano spreading. *Nature* 387, 387–390. doi: 10.1038/387387a0
- van Wyk de Vries, B., Kerle, N., and Petley, D. (2000). Sector collapse forming at Casita volcano, Nicaragua. *Geology* 28, 167–170. doi: 10.1130/0091-7613(2000)028<0167:scfacv>2.3.co;2
- van Wyk, de Vries, B., Self, S., Francis, P. W., and Keszthelyi, L. (2001). A gravitational spreading origin for the Socompa debris avalanche. *J. Volcanol. Geotherm. Res.* 105, 225–247. doi: 10.1016/s0377-0273(00)00252-3
- Vespermann, D., and Schmincke, H. U. (2000). “Scoria cones and tuff rings,” in *Encyclopedia of Volcanoes*, eds B. Houghton, H. Rymer, J. Stix, and S. McNutt (Amsterdam: Elsevier).
- Vezzoli, L., Renzulli, A., and Menna, M. (2014). Growth after collapse: the volcanic and magmatic history of the Neostromboli lava cone (island of Stromboli, Italy). *Bull. Volcanol.* 76, 1–24. doi: 10.1155/2015/434090
- Vidal, N., and Merle, O. (2000). Reactivation of basement faults beneath volcanoes: a new model of flank collapse. *J. Volcanol. Geotherm. Res.* 99, 9–26. doi: 10.1016/s0377-0273(99)00194-8
- Voight, B. (2000). Structural stability of andesite volcanoes and lava domes. *Philos. Trans. R. Soc. Lond. Series A* 358, 1663–1703. doi: 10.1098/rsta.2000.0609
- Walker, D., Stolper, E. M., and Hays, J. F. (1979). “Basaltic volcanism—the importance of planet size,” in *Proceedings of the Lunar and Planetary Science Conference Proceedings*, (New York: Pergamon Press).
- Walker, G. P. (1993). Basaltic-volcano systems. *Geol. Soc. Spec. Publ.* 76, 3–38. doi: 10.1144/gsl.sp.1993.076.01.01
- Walker, G. P., and Sigurdsson, H. (2000). “Basaltic volcanoes and volcanic systems,” in *Encyclopedia of Volcanoes*, eds B. Houghton, H. Rymer, J. Stix, and S. McNutt (Amsterdam: Elsevier).
- Wallace, P. J., Plank, T., Edmonds, M., and Hauri, E. H. (2015). “The encyclopedia of volcanoes,” in *Volatiles in Magmas*, eds H. Sigurdsson, B. Houghton, S. McNutt, H. Rymer, and J. Stix (Amsterdam: Elsevier).
- Walter, T. R., Acocella, V., Neri, M., and Amelung, F. (2005). Feedback processes between magmatic events and flank movement at mount Etna (Italy) during the 2002–2003 eruption. *J. Geophys. Res. Solid Earth* 110, 1–12
- Walter, T. R., Haghghi, M. H., Schneider, F. M., Coppola, D., Motagh, M., Saul, J. (2019). Complex hazard cascade culminating in the Anak Krakatau sector collapse. *Nat. Commun.* 10:4339.
- Walter, T., and Troll, V. R. (2003). Experiments on rift zone evolution in unstable volcanic edifices. *J. Volcanol. Geotherm. Res.* 127, 107–120 doi: 10.1016/s0377-0273(03)00181-1
- Wardman, J., Sword-Daniels, V., Stewart, C., and Wilson, T. (2012). *Impact Assessment of the May 2010 Eruption of Pacaya Volcano, Guatemala*. New Zealand: University of Canterbury. Geological Sciences.
- Watt, S. F. (2019). The evolution of volcanic systems following sector collapse. *J. Volcanol. Geotherm. Res.* 384, 280–303. doi: 10.1016/j.jvolgeores.2019.05.012
- Watt, S. F., Karstens, J., Micallef, A., Berndt, C., Urlaub, M., Ray, M., et al. (2019). From catastrophic collapse to multi-phase deposition: flow transformation, seafloor interaction and triggered eruption following a volcanic-island landslide. *Earth Planet. Sci. Lett.* 517, 135–147 doi: 10.1016/j.epsl.2019.04.024
- Waythomas, C. F., Miller, T. P., and Nye, C. (2003). *Preliminary Geologic Map of Great Sitkin Volcano, Alaska (No. 2003-36)*. US: US Geological Survey.
- White, S. M., Crisp, J. A., and Spera, F. J. (2006). Long-term volumetric eruption rates and magma budgets. *Geochem. Geophys.* 7, 1–20. doi: 10.1002/9781119521143.ch1
- Williams, R., Rowley, P., and Garthwaite, M. C. (2019). Reconstructing the Anak Krakatau flank collapse that caused the December 2018 Indonesian tsunami. *Geology* 47, 973–976 doi: 10.1130/g46517.1
- Wilson, L. (2007). “Planetary Volcanism,” in *Encyclopedia of the Solar System*, 2nd Edn, eds L.-A. McFadden, P. R. Weissman, and T. V. Johnson (Amsterdam: Elsevier).
- Winslow, H., Ruprecht, P., Stelten, M., and Amigo, A. (2020). Evidence for primitive magma storage and eruption following prolonged equilibration in thickened crust. *Bull. Volcanol.* 82, 1–24.
- Witham, C. S. (2005). Volcanic disasters and incidents: a new database. *J. Volcanol. Geotherm. Res.* 148, 191–233. doi: 10.1016/j.jvolgeores.2005.04.017
- Wooller, L., van Wyk de Vries, B., Cecchi, E., and Rymer, H. (2009). Analogue models of the effect of long-term basement fault movement on volcanic edifices. *Bull. Volcanol.* 71, 1111–1131. doi: 10.1007/s00445-009-0289-3
- Xu, Y., Wang, Q., Tang, G., Wang, J., Li, H., Zhou, J., et al. (2020). The origin of arc basalts: new advances and remaining questions. *Sci. China Earth Sci.* 63, 1969–1991. doi: 10.1007/s11430-020-9675-y
- Yamamoto, M. (1988). Picritic primary magma and its source mantle for Oshima-Ōshima and back-arc side volcanoes, Northeast Japan arc. *Contrib. Mineral. Petrol.* 99, 352–359. doi: 10.1007/bf00375367
- Yoshida, H., Sugai, T., and Ohmori, H. (2012). Size-distance relationships for hummocks on volcanic rockslide-debris avalanche deposits in Japan. *Geomorphology* 136, 76–87. doi: 10.1016/j.geomorph.2011.04.044
- Zernack, A. V., and Procter, J. N. (2021). “Cyclic growth and collapse of stratovolcanoes,” in *Volcanic Debris Avalanches: from Collapse to Hazard*, eds M. Roverato, A. Dufresne, and J. Procter (Berlin: Springer).
- Zimelman, D. R., Rye, R. O., and Breit, G. N. (2005). Origin of secondary sulfate minerals on active andesitic stratovolcanoes. *Chem. Geol.* 215, 37–60. doi: 10.1016/j.chemgeo.2004.06.056
- Zobin, V. M. (2001). Seismic hazard of volcanic activity. *J. Volcanol. Geotherm. Res.* 112, 1–14. doi: 10.1016/s0377-0273(01)00230-x

Conflict of Interest: The authors declare that the research was conducted in the absence of any commercial or financial relationships that could be construed as a potential conflict of interest.

Copyright © 2021 Romero, Polacci, Watt, Kitamura, Tormey, Sielfeld, Arzilli, La Spina, Franco, Burton and Polanco. This is an open-access article distributed under the terms of the Creative Commons Attribution License (CC BY). The use, distribution or reproduction in other forums is permitted, provided the original author(s) and the copyright owner(s) are credited and that the original publication in this journal is cited, in accordance with accepted academic practice. No use, distribution or reproduction is permitted which does not comply with these terms.